Describing the vertical root distribution of alpine plants with simple climate, soil, and plant attributes

Describing the vertical root distribution of alpine plants with simple climate, soil, and plant attributes

Alejandro Gonzalez-Ollauri[1*], Csilla Hudek[2], Slobodan B. Mickovski[1], Davide Viglietti[4], Nicole Ceretto[4], Michele Freppaz[3,4]

[1]The BEAM Research Centre, School of Computing, Engineering and Built Environment, Glasgow Caledonian University, Glasgow G40BA, Scotland, UK

[2]Cranfield Soil and Agrifood Institute, Cranfield University, College Road MK43 0AL Bedford UK

[3]Research Centre on Natural Risk in Mountain and Hilly Environments, NatRisk, University of Torino, Largo Paolo Braccini 2, 10095 Grugliasco (TO), Italy

[4]Department of Agricultural, Forest and Food sciences, DISAFA, University of Torino, Largo Paolo Braccini 2, 10095, Grugliasco (TO), Italy

[*]Corresponding author: alejandro.ollauri@gcu.ac.uk

Abstract

The vertical root distribution (VRD) in the soil remains unknown for most plant species, as studying root systems in different pedo-climatic settings is time-consuming and methodologically challenging. Yet, information on the VRD of different vegetation types is essential to understand better the biogeochemical processes occurring at the soil-plant-atmosphere continuum. The aim of this study was to describe the (VRD) of three dominant alpine, herbaceous plants (i.e. *Euphrasia minima* Jacq., *Leucanthemopsis alpina* L., and *Poa alpina* L.) on the basis of simple and easy-to-measure climate, soil, and plant attributes in order to test the validity of existing descriptive protocols and parametric ecohydrological models. The results showed that the VRD decreased with soil depth for the three plants and that it can be effectively described with a negative exponential equation. Key VRD parameters, such as

the mean rooting depth, cross-sectional area at the root collar, and root biomass, were both site and species-specific but they were chiefly influenced by the attributes regulating the soil's water mass balance. The existing parametric ecohydrological models were not able to portray successfully the VRD of the studied alpine plants but we found a strong correlation between empirical and parametric VRD models that establish a clear direction for future research. Future work should address the influence of the snowpack characteristics and the length of the snow-free and frozen ground periods on the soil's ecohydrology and VRD in alpine ecosystems.

Keywords: root, model, ecohydrological, alpine, data mining

Abbreviations

α	Mean precipitation intensity over VSD	θfc	Soil moisture at field capacity
AI	Aridity index	θg	Gravimetric soil moisture content
ALR	Allometry ratio	θwp	Soil moisture at wilting point
Ar	Root cross-sectional area	ρ_{bk}	Soil's bulk density
Aro	Cross-sectional area at root collar	ρ_r	Root mass density
b	Mean rooting depth	Sa	Soil's sand content
Cl	Soil's clay content	Sk	Soil skeleton
CN	Concave topographic curvature	SOC	Soil organic carbon
CS	Plant's crown spread	Sp	Plant's aerial projected area
CX	Convex topographic curvature	Tbase	Optimum temperature for plant growth
Etp	Potential evapotranspiration	Tmn	Daily minimum air temperature
FL	Flat topographic curvature	Tmx	Daily maximum air temperature
GDD	Growing-degree day	VRD	Vertical root distribution
λ	Precipitation frequency over VSD	VSD	Vegetative season duration
Ma	Aboveground biomass	WAP	Water available to plants
Mr	Belowground biomass	z	Soil depth
n	Soil porosity		

1. Introduction

Knowledge of root systems of different vegetation types is essential for a better understanding of biogeochemical processes occurring at the soil-plant-atmosphere continuum (Rodriguez-Iturbe and Porporato, 2005). Despite relatively recent efforts in investigation and description of plant root architecture (e.g., Waisel et al., 2002, Mickovski and Ennos 2003, Mickovski and van Beek 2005), it remains largely unexplored for most plant species. A number of authors have explored root system architecture of a large number of plants native to almost all bioclimatic regions (e.g. Schenk and Jackson, 2005), and attempted prediction of rooting depths through optimisation (van Wijk and Bouten, 2001; Kleidon, 2004) or inverse methods (Zuo and Zhang, 2002). These approaches led to an increase in knowledge and understanding of plant physiological processes such as water and nutrient uptake, resources competition, and plant-soil interactions (Herbert et al., 2004; Laio et al., 2006, Preti et al., 2010; Gonzalez-Ollauri and Mickovski, 2017a). Despite the efforts in the past decade, the comprehensive understanding of the effect of soil and plant properties and climate conditions on root architecture and morphology remains largely unknown.

Obtaining root information is time-consuming and methodologically challenging. The investigation of root systems normally involves destructive and invasive sampling approaches (Bhöm, 1979), followed by detailed description and measurement of specific root traits (Stokes et al., 2009). However, for many environmental applications related to plant-soil interactions, knowledge of the vertical root distribution (VRD) – i.e. the pattern in which root density biomass is distributed along the soil profile - is perhaps the most important feature to know

because it can be used, for example, to estimate the degree of soil-root mechanical reinforcement (Arnone et al., 2016; Gonzalez-Ollauri and Mickovski, 2016; Kokutse et al., 2016), to estimate plant-water uptake (Jarvis, 1989; Laio, 2006; Shukla, 2014), or to gain insight into the ability of vegetation to remove pollutants from the soil (Verma et al., 2006; Gonzalez-Ollauri and Mickovski, 2018; Lucherini et al., 2020). For most of these applications, VRD can be easily portrayed with asymptotic mathematical functions (Jackson et al., 1996), which substantially simplify the process of describing the root system, as they normally require few parameters related to the root system, such as the rooting depth or the cross-sectional area at the root collar (Preti et al., 2010). However, standard and reproducible protocols to describe VRD are still lacking.

The way in which roots distribute in the soil has been the scope of research for many decades (e.g. Darwin, 1880; Laio et al., 2006). Previous research indicates that the root distribution in the soil is mostly influenced by water availability to plants (i.e. hydrotropism; Tsutsumi et al., 2003). This is relevant because it permits to connect VRD to climate and soil attributes regulating the water cycle in the soil (e.g. soil porosity, soil organic matter, soil texture, etc; Toth et al., 2015), and to set the basis for establishing cost-effective analytical approaches describing VRD on the basis of few, easy-to-measure variables. As a result, and to the best of our knowledge, two parametric, ecohydrological models predicting VRD have been developed for arid or semi-arid (Laio et al., 2006; Preti et al., 2010) and for temperate-humid (Gonzalez-Ollauri and Mickovski, 2016) ecosystems, respectively. These models incorporate plant-specific attributes by considering the relative allocation of plant biomass between the above- and belowground soil compartments (i.e. allometry; Cheng and Niklas. 2007) and by assuming that the root system can take a known, simple geometrical shape, such as a cylinder, a cone, or a hemisphere (e.g. Lynch, 1995; Kutschera and Lichtenegger, 1992; Kokutse et al., 2006). The

ability of these models to realistically portray VRD has been successfully tested for few herbaceous (Gonzalez-Ollauri and Mickovski, 2016) and shrub species (Preti and Giadrossich, 2009; Preti et al., 2010), but their application to the wider pool of plants, in general, and to woody plants (e.g. Preti et al., 2010; Tron et al., 2014; Tardio et al., 2016), in particular, needs further validation. In addition, the robustness of the model conceptualisation and the assumptions still need to be verified against primary data showing the influence of multiple soil and plant attributes on VRD, which could help to identify potential model improvements including application to climates with different ecohydrological features, such as tropical or alpine.

Alpine ecosystems are normally found above the upper limit of tree growth in mountainous areas. They are generally characterised by cold winter temperatures, precipitation in the form of snow, and short snow-free periods (Freppaz et al., 2019) – all of which tend to limit the duration of the vegetative season. As a result, alpine vegetation, which mostly comprises low-growing herbaceous perennial plants, tends to be sparse and endemic to these ecosystems, or it may have evolved to withstand the environmental stress related to alpine climates (Germino, 2014). In addition, the growth and development of alpine plants is also constrained by the low availability of nutrients in the soil, particularly nitrogen (e.g. Freppaz et al., 2019; Zong et al., 2020). Still, alpine vegetation may play a crucial role in cycling carbon and nutrients in alpine ecosystems (e.g. Iversen et al., 2014), or in protecting the soil against shallow landslides and erosion (Preti. 2013; Burylo et al., 2014; Gonzalez-Ollauri and Mickovski, 2017b), where poorly developed soils subjected to freezing are prone to soil mass wasting processes (e.g. Hudek et al., 2017a). Yet, knowledge of the root systems in alpine plants is scarce (e.g. Iversen et al., 2014) and only few studies have attempted addressing this knowledge gap (e.g. Pohl et al., 2011; Burylo et al., 2014; Hudek et al., 2017b).

The aim of this study is to describe the VRD of three dominant alpine plants on the basis of simple and easy-to-measure climate, soil, and plant attributes in order to test existing descriptive protocols and parametric ecohydrological models. The objectives of the study include (i) selection and characterisation of three alpine sites in terms of climate and soil attributes, (ii) sampling above- and below-ground plant parts of three dominant pioneer plant species from the three study locations to retrieve relevant plant information and to describe the VRD, (iii) investigation of the influence of evaluated soil and plant attributes on key VRD parameters, and (iv) testing the predictive capacity of an existing parametric ecohydrological model for VRD using pedo-climatic and plant attributes.

2. Materials and Methods

2.1. Study area

The study area is located adjacent to Monte Rosa massif (4634 m above sea level; a.s.l.), within the Long-Term Ecological Research (LTER) site Angelo Mosso Institute, Valle d'Aosta Region, Northwest Italy (Fig. 1a). The climate in the study area is Alpine (ET; Köppen, 1884), characterised by a mean annual air temperature of -2.5°C, a cumulative annual snowfall of 8.50 m, and a mean annual rainfall of 350 mm. The snowpack generally develops in late October - early November and lasts until the onset of snowmelt in late May – early June. Soil temperature and meteorological parameters such as air temperature, rainfall during the snow-free season, and snowfall have been continuously recorded with a 1-minute resolution in the study area since 2005 using one Automatic Weather Station (AWS) located at 2901 m a.s.l. (Fig. 1; Comando Truppe Alpine - Servizio Meteomont).

Three, high-altitude study sites located in the upper part of a glacier valley were selected within the study area (Fig. 1a). The sites were located at different elevations and had distinct underlaying soil types -i.e. Site 1: 2840 m a.s.l on Dystric Leptic Regosol; Site 2: 2795 m on Dystric Lithic Leptosol ; Site 3: 2770 m on Haplic Umbrisol (IUSS Working Group WRB, 2015). Sites 1 and 2 (Figs.1b and 1c) are characterised by relatively flat topographies. The dominant vegetation at these sites comprises nival plant species of perennial grasses (*Poa laxa, Poa alpina),* together with other herbaceous species such as forbs (*Leucanthemopsis alpina, Gnaphalium supinum*), cushion plants (*Minuartia sedoides*) and dwarf, woody plants that can tolerate long-lasting snow cover (*Salix herbacea, Loiseleuria procumbens*). The topography of Site 3 is rougher and the vegetation cover denser than at sites 1 and 2 (Fig. 1a). Alpine grasslands dominate Site 3 with the most characteristic plant species being *Carex curvula* and *Euphorbia minima* (Freppaz et al., 2019; Lonati et al., unpublished data).

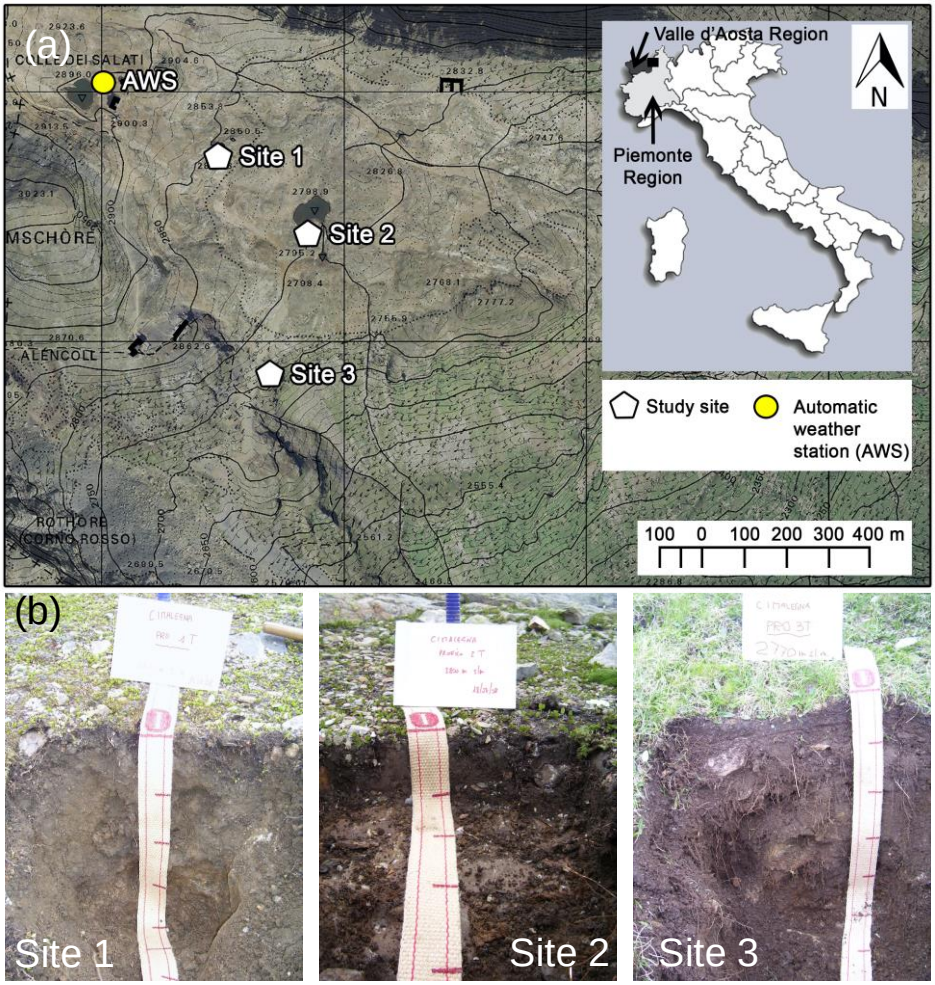

Figure 1 a) Locations of the study sites (1-3) and b) characteristic soil profiles for site 1, 2 and 3.

2.2.Climatic attributes

We measured four climatic attributes reported to influence plant growth and root development (e.g. Preti et al., 2010; Gonzalez-Ollauri and Mickovski, 2016), and which are nested in the parametric, ecohydrological VRD model to be tested herein (Section 2.6; Table 1). To this end, we examined daily meteorological records collected with one AWS between 2005 and 2019 (Fig. 1a), which we assumed to be representative for the three study sites. The vegetative season duration (VSD) was defined using the heuristic growing-degree days (GDD; Eq.8) approach (e.g. McMaster and Wilhelm, 1997), which is a measure of the daily heat accumulation to

predict plant development and phenology. We assumed that the vegetative season begun once the cumulative GDD reached 200˚C (Eq.8; Table 1), and that it ended when daily mean soil temperature was below 4˚C (i.e. root growth is inhibited under 4˚C; e.g. Alvarez-Uria and Körner, 2007). We also assumed 5˚C as the optimum soil temperature for plant growth (*Tbase*; Eq.8; Table 1). We then calculated the aridity index (*AI*) of the study site as the ratio of the total potential evapotranspiration to the total precipitation (Eq. 9; Table 1; Greve et al., 2019) over the vegetative season. The total precipitation was considered as the sum of rainfall and snowfall (i.e. snow water equivalent) recorded during the vegetative season of each examined year. The total potential evapotranspiration over the vegetative season, which is in turn nested in the VRD model (Eq.4; Table 1), was calculated with the Priestly and Taylor (1972) equation (Eq. 10; Table 1). Subsequently, we estimated the mean precipitation depth (α; mm event^{-1}) and the frequency of precipitation events (λ) during the vegetative season (Laio et al., 2006; Preti et al., 2010). We calculated α as the ratio of the total precipitation to the number of precipitation events (i.e. days with precipitation > 0.2 mm) during the vegetative season averaged for the studied time period comprised between 2005 and 2019. Rainfall lost to surface runoff was assumed to be negligible in our study area (e.g. Tron et al., 2014). We calculated λ as the ratio of the number of precipitation events to the total vegetative season duration averaged for the studied period.

2.3.Soil attributes

The slope gradient and aspect were measured manually with a hand-held inclinometer and with a compass, respectively, at locations adjacent to each sampled plant individual (Section 2.4). The terrain curvature of each sampling location was visually described as either concave (CN), convex (CX) or flat (FL) (e.g. Gonzalez-Ollauri and Mickovski, 2017c). Undisturbed soil

samples (N=36) from the topsoil (0 mm - 100 mm below ground level; b.g.l) were collected at the same locations where plants were sampled using a soil core sampler. These samples were used to determine the soil bulk density (ρ_{bk}; g cm^{-3}), soil porosity (n) and gravimetric moisture content (θ_g; %) following standard methods (Head, 1980). The soil organic carbon (*SOC*; %) and *pH* were determined using a portion of the collected soil materials, which was air-dried for 168 h and sieved through a 2 mm opening sieve. *SOC* was determined using a C/H/N analyser (Elementar Vario EL) while soil pH was determined in soil–water suspension (soil: water = 1:2.5) following the slurry method (ASTM, 1995) and using a *pH* electrode (Fisher Scientific Accumet Basic AB15). Additional soil materials in form of bulk samples of 4kg-5kg were collected with a shovel from the topsoil (0 mm – 300 mm b.g.l) at three representative locations per study site (N=9). These representative sampling locations, which were assumed to capture the main soil features within a study site, were within the area range covered by plant sampling, and were less than 5 m away from any given plant individual sampled in this study. The soil samples were stored in heavy-duty PVC bags and transported to the laboratory where they were mixed per study site (N=3) prior to further analysis. The particle size distribution (PSD) of the collected soil materials was determined through the dry sieving and the hydrometer methods for the coarse (i.e. gravel and sand) and fines (i.e. silt and clay) fractions, respectively (Head, 1980). The soil skeleton (i.e. percentage of rock fragments in the soil sample; *Sk*; %) was determined through dry sieving (Head, 1980). Soil moisture content at field capacity (θfc; %) and wilting point (θwp; %) were estimated through pedotransfer functions (Eqs. 11 and 12; Table 1; Toth et al., 2015), which are nested in the VRD model and use PSD, *n*, and *SOC* as inputs.

2.4. Plant species, plant attributes and vertical root distribution

We selected three dominant, characteristic plant species for the study from sites 1, 2, and 3 (Fig.1):

(i) dwarf eyebright (*Euphrasia minima* Jacq.), an annual, facultative root hemiparasite (Matthies, 1998; Fig. 2a) with erect stems reaching up to 150 mm, which grows in humid mountainous habitats between 950-3000 m a.s.l. (Asturnauta, 2020)

(ii) alpine chrysanthemum (*Leucanthemopsis alpina* L.), a perennial, herbaceous plant belonging to the daisy family and specific to high alpine elevations, growing between 1800-3500 m a.s.l. It can be an early coloniser after the retreat of glaciers, being generally small in size (< 200 mm in height) with a root system characterised by horizontal rhizomes (ukwildflowers.com, 2020; Fig. 2b).

(iii) alpine bluegrass (*Poa alpina* L.), a subartic-alpine meadow tufted grass found in moist to dry limestone and in basaltic rock crevices and exposed heathlands. It is a pseudoviviparous, apomictic, and fast germinating plant (Pierce et al., 2000) that can reach up to 400 mm in height, normally has narrow leaves (2-4 mm), and its inflorescence is pyramidal, twice as tall as wide; it also has an adventitious root system that arises extra-vaginally through the lead-sheaths at the base of the plant (Pierce et al., 2000; Fig. 2c).

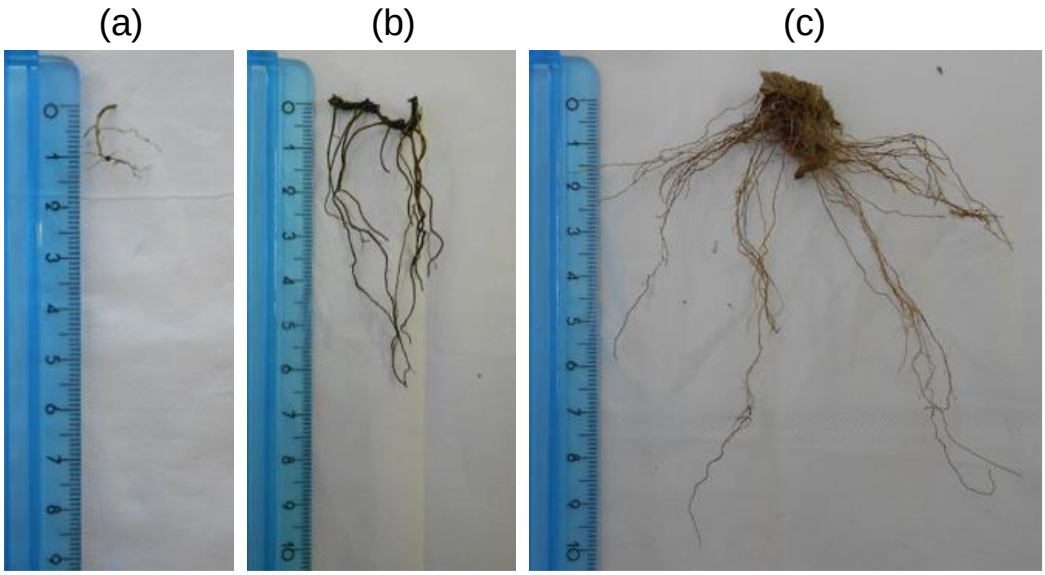

Figure 2. Selected root systems of (a) Euphrasia minima (b) Leucanthemopsis alpina (c) Poa alpina.

Plant sampling was undertaken at the height of the growing season when four individuals per plant species were sampled at random locations within each study site (N=36; Fig. 1). The projection area of the aerial plant parts (*Sp*; cm^2; total plant aboveground area projected on the ground, assuming a plant crown with a circular shape) and average crown spread (*CS*; cm; mean spread diameter of the aboveground plant parts) were measured for each sampled individual with a meter tape following the Spokes distance method (Blozan, 2006). Each plant individual was excavated by hand before being clipped with scissors above the root collar (Fig. 3) to separate the above from the belowground part. The aboveground plant materials were oven-dried at 60˚C until constant mass to measure the aboveground biomass (*Ma*; g) of each sampled individual. The belowground parts were cleaned with a water jet to separate soil particles attached to the root system prior to being air-dried for 2 h for describing the vertical root distribution (VRD).

VRD was measured manually as the total cross-sectional root area at a given soil depth (Fig. 3) for each sampled plant before being averaged per plant species and study site. Using a permanent marker and a ruler, marks were drawn on the root systems at equal length intervals

ranging from 5 to 20 mm and starting from the root collar (Fig. 3) to visualise the assumed root-soil intersection planes (Fig. 3). The diameter of all the roots intersecting each plane was measured with Vernier callipers, and their cross-sectional area (*Ar(z)*; mm^2) was calculated with Eqs. 1 and 2 (Table 1; Fig. 3), assuming all roots had circular cross-section when crossing a given intersection plane (Fig. 3). Subsequently, *Ar* was averaged per intersection plane and per plant species for a given sampling site. Then, a nonlinear least squares (nls) exponential model of the form $y = ae^{-x/b}$, where *y* is the dependent variable (i.e. root cross-sectional area; *Ar*), *x* is the independent variable (i.e. soil depth), and *a* and *b* are fitting parameters (Eq.3; Table 1) was fitted to the measured data resulting from the previous step. With this approach and, for modelling purposes, it was assumed that the root biomass is distributed in the soil following a cone shape volume (Fig. 3b; Preti et al., 2010; Gonzalez-Ollauri and Mickovski, 2016; see Supplementary Material) in which the total rooting depth (i.e. soil depth at which 95 % of roots are found; 3x*b*; mm; Laio et al., 2006) was the cone's height and the cross-sectional area of the root collar (*Aro*; mm^2) the cone's basal area (Fig. 3b). Accordingly, the rooting depth (*b*; mm) was quantified as 1/3 of the longitudinal distance between the root collar and the tip of the root system of each studied individual (Laio et al., 2006). It must be borne in mind that with the former cone-shape-volume approach (Fig. 3b), we are not trying to capture the shape of the root system *per se* (Fig. 2; e.g. Köstler et al., 1968) but to provide a generic basis to model the widely-observed decrease in root biomass with soil depth (e.g. Schenk, 2005; see Supplementary Material). Finally, the root materials were oven-dried at 60°C until constant mass to measure the root biomass (*Mr*; g) and the allometry ratio (*ALR*) as the quotient between *Mr* and *Ma*.

Table 1. List of equations used in this study. Arid and humid ecosystems are defined on the basis of the aridity index (AI) over the growing season -i.e. AI < 1: arid; AI > 1: humid; ppu: parts-per unit. VS: vegetative season.

Definition	Equation	No	Parameters	Units	Source
Cross-sectional area of the ith root at a given intersection plane	$Ai = \pi\,(dx/2)^2$	Eq. 1	*Ai*: cross-sectional area of the ith root at a given intersection plane *dx*: root diameter	mm^2 mm	Gonzalez-Ollauri and Mickovski (2016)
Root cross-sectional area at a given intersection plane	$Ar(z_i) = \Sigma Ai$	Eq.2	*Ar(z$_i$)*: cross-sectional area of all roots crossing a given intersection plane	mm^2	Gonzalez-Ollauri and Mickovski (2016)
Vertical root distribution (VRD)	$Ar(z) = Aro.e^{\frac{-z}{b}}$	Eq. 3	*Ar(z)*: cross-sectional area of all roots along the soil profile *Aro*: cross-sectional area of the plant stem above the root collar *b*: mean rooting depth *z*: soil depth	mm^2 mm^2 mm mm	Preti et al. (2010)
Mean rooting depth in arid and semi-arid ecosystems	$b = \frac{\alpha}{n(\theta fc - \theta wp)(1 - \frac{\lambda\alpha}{Etp})}$	Eq. 4	α: mean precipitation intensity per event over the growing season n: soil porosity θfc: volumetric soil moisture content at field capacity	mm event^{-1} ppu ppu	Laio et al. (2006)

			θwp: columetric soil moisture content at wilting point *λ:* frequency of precipitation events over the growing season *Etp*: total potential evapotranspiration over the growing season	ppu events mm	
Mean rooting depth in humid ecosystems	$b = \frac{\alpha}{n(\theta fc - \theta wp)}$	Eq. 5			Gonzalez-Ollauri and Mickovski (2016)
Water available to plants in the soil	$WAP = \theta fc - \theta wp$	Eq. 6	*WAP*: water available to plants	ppu	
Area at the root collar	$Aro = \frac{Mr}{b\ \rho r}$	Eq. 7	*Aro*: cross-sectional area of the plant stem above the root collar *Mr*: plant belowground biomass ρr: root mass density	mm^2 g $g\ mm^{-3}$	Preti et al. (2010)
Growing-degree day	$GDDi = \frac{Tmx - Tmn}{2} - Tbase$	Eq.8	*Tmx:* daily maximum air temperature *Tmn*: daily minimum air temperature	ºC	McMaster and Wilhelm (1997)

	$\begin{cases} \sum_{i=1}^{n} GDDi \geq 200℃. & VS\ start \\ Tsoil \leq 4℃ & VS\ end \end{cases}$		*Tbase:* optimum daily mean temperature for plant growth *i*: ith day *Tsoil*: daily mean soil temperature	°C °C	
Aridity index	$AI = \frac{Etp}{PCP}$	Eq. 9	*PCP*: total precipitation over the growing season	mm	Greve et al. (2019)
Potential evapotranspiration	$Etp = 0.00128 \frac{Rnl}{58.3} \frac{\Delta}{\Delta + \gamma}$	Eq. 10	*Rnl*: net solar radiation Δ: slope of saturation vapour pressure γ: psychrometric constant	MJ m^{-2} day^{-1} kPa °C kPa °C	Priestly and Taylor (1972)
Soil moisture at field capacity	$\theta fc = \theta_{33} + 1.23{\theta_{33}}^2 - 0.374\theta_{33} - 0.015$ $\theta_{33} = -0.251Sa + 0.195Cl + 0.011SOC + 0.006Sa.SOC - 0.027Cl.SOC + 0.452Sa.Cl + 0.299$	Eq. 11	θ33: soil moisture at -33 kPa of matric suction Sa: sand content in the soil Cl: clay content in the soil SOC: soil organic carbon	ppu ppu ppu ppu	Toth et al. (2015)
Soil moisture at wilting point	$\theta_{wp} = \theta_{1500} + 0.14\theta_{1500} - 0.02$ $\theta_{1500} = -0.024Sa + 0.487Cl + 0.006SOC + 0.005Sa.SOC - 0.013Cl.SOC + 0.068Sa.Cl + 0.031$	Eq. 12	θ1500: soil moisture at -1500 kPa of matric suction	ppu	Toth et al. (2015)

283

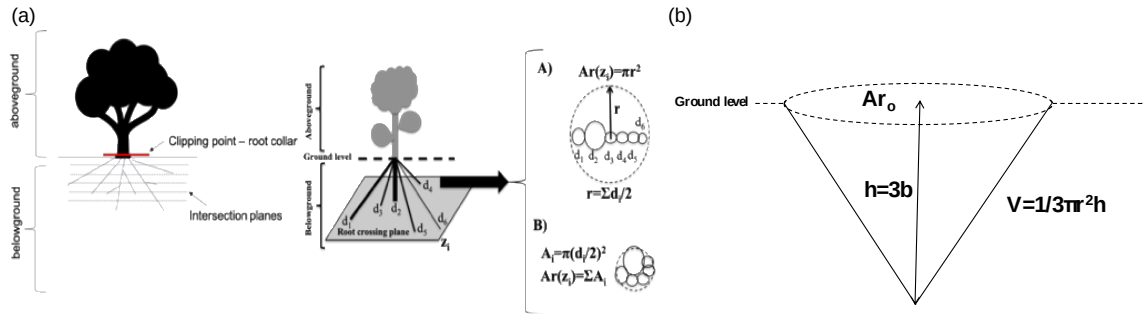

Figure 3. (a) Illustration of the methodological approach followed to separate aboveground and belowground plant parts and to describe vertical root distribution (VRD) for the studied plant species. Approach B was followed to describe the cross-sectional area of all roots at a given crossing plane (Ar(z)) , as it does not overestimate the root cross-sectional area compared to approach A. r stands for the rooting radius and d for the diameter of ith root at a given crossing plane. (b) VRD was modelled as a cone with base's area Aro (i.e. root collar area; mm²) and height 3b, being b the mean rooting depth (mm) and 3b the soil depth at which 95% of the roots are found (Laio et al., 2006). V stands for the cone volume and h for the cone height. See mathematical formulation in Supplementary Material.

2.5. Relationship between soil and plant attributes with key VRD parameters

We investigated the relationship between the studied soil (Section 2.3) and plant attributes (Section 2.4) with the relevant/key parameters used to portray VRD (*Aro*: cross-sectional area of the root collar, and *b*: mean rooting depth) through a data mining workflow (Supplementary Material – Fig. S1) which was built using the statistical language R v5.5.1 (R Core team, 2018). We also included plant belowground biomass (*Mr*) in the analysis, as *Mr* will ultimately limit the extent of VRD (Gonzalez-Ollauri and Mickovski, 2016). This workflow was used to accomplish three objectives: (i) to evaluate the ability to predict relevant VRD parameters using the investigated soil and plant attributes as predictors, (ii) to evaluate the importance of

each plant and soil predictor on the relevant VRD parameters, and (iii) to evaluate predictor-response dependency - i.e. how the response variable changes following predictor changes.

To accomplish objective (i), 100 random forest models (RF; Breiman, 2001) were fitted with 1000 regression trees each, using the R package "randomForest" (Liaw and Wiener, 2020). Only uncorrelated attributes to the VRD parameters were considered to fit RF models. Each RF model was cross-validated with a bootstrapping method without replacement (e.g. Gonzalez-Ollauri et al., 2020) and through the evaluation of the coefficient of determination (R^2), root mean square error (RMSE) and variance explained (VExp) following the least-squares method (Fuller, 1987). The pool of cross-validation coefficients retrieved from implementing the data mining workflow was examined by plotting their corresponding probability density functions (Appendix A).

To accomplish objective (ii), the importance of each plant and soil attribute on the response variables (i.e. key VRD parameters) was examined on the basis of permutation tests using the R package "caret" (Khun et al., 2018), which measures attribute importance by observing model performance when each predictor is randomly dropped out from fitting a RF model during the training step (e.g. Strobl et al., 2008).

To achieve objective (iii), we examined the Partial Dependence Plots (PDPs; Hastie et al., 2009) retrieved from using the R package "pdp" (Greenwell, 2017). PDPs were retrieved to show whether the interaction between a target VRD parameter and a target plant and soil attribute was linear, monotonic, or more complex in the fitted RF models, representing how a given attribute influenced the prediction on average for a given VRD parameter. The R script used to implement the data mining workflow described above is provided in Appendix C.

330

331 2.6. Empirical vs. parametric, ecohydrological model for vertical root distribution

332

333 We tested the predictive capacity of an existing parametric ecohydrological model for vertical
334 root distribution (Eqs. 4-5, Table 1; Laio et al. 2006; Preti et al., 2010; Gonzalez-Ollauri and
335 Mickovski, 2016) against the empirical VRD model fitted to the measured data described in
336 Section 2.4. The parametric ecohydrological VRD model was firstly developed for arid and
337 semi-arid ecosystems by Laio et al. (2006) and extended by Preti et al. (2010), and then adapted
338 to temperate-humid climates by Gonzalez-Ollauri and Mickovski (2016). This model estimates
339 the mean rooting depth (*b*; Eqs. 4 and 5; Table 1) on the basis of pedo-climatic parameters (i.e.
340 α: mean precipitation depth during the growing season; λ: frequency of precipitation events;
341 *Etp*: potential evapotranspiration; Section 2.2) and of the product between soil porosity (*n*) and
342 the water available to plants in the soil (*WAP*; Eq. 6; Table 1), function of the difference
343 between the volumetric soil moisture content at field capacity (θ_{fc}) and at wilting point (θ_{wp}).
344 Different equations for *b* must be considered depending on whether the aridity index (*AI*; Eq.
345 8) is greater than 1 (i.e. arid climate; Eq. 4; Preti et al., 2010) or lower than 1 (i.e. humid
346 climate; Eq.5; Gonzalez-Ollauri and Mickovski, 2016). VRD is then modelled with a negative
347 exponential equation (Eq. 5; Table 1) using *b*, the cross-sectional area at the root collar (*Aro*)
348 and the soil depth (*z*; mm) as inputs, assuming that the probability density function for the daily
349 rainfall intensity at the study site is exponentially distributed (Laio et al., 2006). The cross-
350 sectional area at the root collar (*Aro*) is estimated using plant-specific information and the
351 rooting depth under the assumption that the distribution of root biomass along the soil profile
352 can be portrayed with a conical-shape-volume (Fig. 3b; Section 2.4; Eq. 6; Table 1;
353 supplementary material). In addition, we assumed that the portion of soil explored by roots was
354 uniform and isotropic.

The outcomes from the parametric, ecohydrological and the empirical VRD models were compared in the light of the outputs for the root cross-sectional area (*Ar*) of all roots along the soil profile. To do so, *Ar* was firstly retrieved for soil depths of 0 mm - 100 mm using the parametric ecohydrological and empirical VRD models (Section 2.4), respectively. Then, the two *Ar* datasets were log-transformed and plotted together to graphically evaluate the mathematical relationship between the two models. Subsequently, a linear regression model was fitted between the two retrieved, log-transformed *Ar* datasets in R v3.5.1. Additionally, the correlation between the linear fitting parameters and the studied plant and soil attributes was examined by estimating pairwise Pearson's correlation coefficients.

2.7. Statistical analysis

Normality checks were undertaken for every studied soil and plant attribute with the Shapiro Wilk test. Soil and plant attributes were aggregated into plant species and study site, respectively, for statistical analysis. Statistical differences in plant attributes between plant species and investigation site were evaluated with the non-parametric Kruskal Wallis (χ^2) test, as plant attributes did not follow a normal distribution. Where statistically significant differences were encountered, plant attribute's differences between two plant species were evaluated with the non-parametric Wilcoxon (W) test. Statistical differences in soil attributes between plant species and investigation site were evaluated with one-way ANOVA (F) and Kruskal Wallis (χ^2) tests for normal and non-normal distributed variables, respectively. Vertical root distribution (VRD) differences between investigated sites were evaluated per plant species with the Kruskal Wallis (χ^2) test, as VRD did not follow a normal distribution. Where statistically significant differences were encountered, the differences within the plant

species were evaluated with the non-parametric Wilcoxon (W) test. VRD differences between plant species for a given investigation site were examined with the same approach indicated before. Statistical differences between the importance of the attributes used as predictors for the selected VRD parameters were also evaluated with the Kruskal Wallis test. The statistical relationship between the studied plant and soil attributes was evaluated with the pair-wise Pearson's correlation test and interpreted on the basis of the resulting correlogram plot. All statistical tests were carried out at the 95 % and 99 % confidence level using the 'base' package embeddedw in the statistical computing software R v3.5.1 (R Core Team, 2018).

3. Results

3.1. Climate attributes

The growing season duration for the period 2005-2019 was on average 50±18 days long, generally starting in early July and ending in early September. The aridity index of the study site during the snow-free period was 0.91±0.2, indicating that the temperate-humid, ecohydrological VRD model (Eq.5; Table 1) must be implemented for the study area. The mean precipitation depth per event during the growing season (α) was 6.68±2.33 mm, the frequency of precipitation events (λ) was 0.56±0.05, and the total potential evapotranspiration (*Etp*) during the vegetative season was 68.8±2.1 mm.

3.2.Soil attributes

The examined soil attributes (Table 2) differed significantly between the investigated study sites. Site 3 had a substantially higher slope gradient (χ^2:18.2 df:2 $p<0.01$), it was consistently

concave in terms of the terrain curvature, and it had a more South-facing aspect than Sites 1 and 2. In addition, Site 3 had a significantly higher soil moisture ($F:65.89$ $df:1$ $p<0.01$), soil organic carbon ($F:45.3$ $df:1$ $p<0.01$), and proportion of fine soil materials ($\chi^2:35$ $df:2$ $p<0.01$) than Sites 1 and 2, while having a substantially lower bulk density ($\chi^2:20.2$ $df:2$ $p<0.01$), soil skeleton ($\chi^2:35$ $df:2$ $p<0.01$), and coarse soil materials ($\chi^2:35$ $df:2$ $p<0.01$) than the other two

Table 2. Soil attributes investigated in this study averaged per plant species and per sampling site ± standard deviation. θg: gravimetric moisture content; ρ_{bk}: dry bulk density; n: soil porosity; SOC: soil organic carbon; Sk: soil skeleton.

		Slope (°)	*Curvature*	*Aspect*	θg (%)	ρ_{bk} (g cm^{-3})	*n*	*SOC* (%)	*pH*	*Sk* (%)
Plant species	*Euphrasia minima*	8.42±8.7	convex	145.42±22.8	29.20±11.4	1.18±0.2	0.56±0.1	7.70±2.6	4.50±0.1	20.70±7.2
	Leucanthemopsis alpina	8.42±6.3	flat/convex	145±25.3	27.46±9.3	1.24±0.2	0.53±0.1	6.59±1.4	4.50±0.1	20.70±7.2
	Poa alpina	11.50±7.3	flat/convex	152.08±18.8	27.43±9.2	1.20±0.2	0.55±0.1	7.83±2.6	4.50±0.1	20.70±7.2
Sampling site	Site 1	6.92±4.5	flat/convex	133.50±11.1	19.44±7.1	1.37±0.2	0.48±0.1	5.52±1.4	4.60±0.0	16.30±0.0
	Site 2	4.33±2.1	convex	135.5±9.81	26.05±4.0	1.26±0.1	0.52±0.0	6.96±1.4	4.40±0.0	30.40±0.0
	Site 3	17.08±7.3	concave	173.5±14.9	38.60±5.5	0.98±0.2	0.63±0.1	9.64±1.6	4.50±0.0	15.40±0.0

Table 2 Cont. Soil attributes investigated in this study averaged per plant species and per sampling site ± standard deviation. θfc: volumetric soil moisture content at field capacity; θwp: volumetric soil moisture content at wilting point.

		Clay (%)	Fine silt (%)	Coarse silt (%)	Fine sand (%)	Coarse sand (%)	θfc (%)	θwp (%)
Plant species	*Euphrasia minima*	1.40±0.34	5.67±1.11	11.30±3.33	50.73±3.64	30.87±2.15	27.851±0.3	1.56±0.04
	Leucanthemopsis alpina	1.40±0.34	5.67±1.11	11.30±3.33	50.73±3.64	30.87±2.15	28.33±0.2	2.01±0.10
	Poa alpina	1.40±0.34	5.67±1.11	11.30±3.33	50.73±3.64	30.87±2.15	29.18±0.4	3.09±0.20
Sampling sites	Site 1	1.00±0.0	4.30±0.0	9.20±0.0	52.30±0.0	33.20±0.0	28.78±0.7	2.37±0.9
	Site 2	1.40±0.0	5.80±0.0	15.80±0.0	45.90±0.0	31.20±0.0	28.10±0.6	2.20±0.7
	Site 3	1.80±0.0	6.90±0.0	8.90±0.0	54.00±0.0	28.20±0.0	28.23±0.9	2.16±0.7

419 investigated sites (Table 2). However, significant differences for the investigated soil attributes
420 were not detected between the three studied plant species (Table 2; F:1.1 df:2 p=0.34). The
421 available water to plants in the soil (Eq. 6, Table 1) was on average of 26.13±0.3 %.
422
423 3.3.Plant attributes
424
425 The evaluated plant attributes (Table 3) were statistically different between the three studied
426 plant species. In particular, *Poa alpina* individuals had a substantially larger crown spread (CS;
427 χ^2:26.7 df:2 p<0.01), plant projected area (*Sp*; χ^2:26.7 df:2 p<0.01), cross-sectional area at the
428 root collar (*Aro*; χ^2:27.1 df:2 p<0.01), aboveground biomass (*Ma*; χ^2:26.4 df:2 p<0.01), and
429 root biomass (*Mr*; χ^2:29.3 df:2 p<0.01) than those of the other two studied species (Table 3).
430 However, the measured mean rooting depth (*b*) was not statistically different between the three
431 studied plant species (Table 3; χ^2:0.6 df:2 p=0.76). On other hand, the three investigated study
432 sites did not present statistical differences in terms of the evaluated plant attributes (χ^2:0.3 df:2
433 p=0.85) with the exception of the observed *b*, which was significantly higher in Site 3 than in
434 Sites 1 and 2 (Table 3; χ^2:26.7 df:2 p<0.01).
435
436 3.4. Vertical root distribution
437
438 The measured vertical root distribution (VRD) decreased exponentially with soil depth for the
439 three studied plant species and at the three study sites (Fig 5). As a result, negative exponential
440 models (Eq. 3. Table 1) were successfully fitted to the observed data (i.e. empirical model)
441 with high goodness of fit (R^2>0.9) in all cases. The model fitting parameters (Table 4) did not
442 differ statistically from the measured VRD parameters (b:W=49

Table 3. Plant attributes investigated in this study averaged per plant species and per sampling site± standard deviation . CS: crown spread; Sp: plant's aerial projected area; Aro: root collar area; b: mean rooting depth; Ma: aboveground biomass; Mr: root biomass; ALR: allometry ratio -i.e. Mr/Ma.

		CS (cm)	*Sp* (cm^2)	*Aro* (mm^2)	*b* (mm)	*Ma* (mg)	*M*r (mg)	*ALR*
Plant species	*Euphrasia minima*	1.60±1.4	3.44±7.9	0.17±0.1	15.00±10.9	13.38±12.1	1.08±1.1	0.12±0.2
	Leucanthemopsis alpina	3.84±0.8	12.09±4.9	0.38±0.1	14.44±10.9	85.43±40.8	62.12±21.0	0.82±0.4
	Poa alpina	8.01±3.0	56.90±45.7	1.15±0.7	15.83±8.1	226.42±162.4	379.07±366.3	1.82±1.2
Sampling sites	Site 1	4.06±3.3	20.99±31.4	0.72±0.9	4.72±1.9	100.10±132.3	189.71±371.1	1.09±1.1
	Site 2	3.90±2.2	15.49±13.8	0.45±0.4	16.67±7.8	133.03±173.3	158.17±274.4	0.95±1.1
	Site 3	5.49±4.1	35.94±50.5	0.52±0.5	23.89±6.0	92.11±72.5	94.39±142.9	0.71±0.9

Table 24. Vertical root distribution (VRD) parameters measured, retrieved though fitting nls exponential models to the measured data -i.e. empirical VRD model (†), and predicted with the parametric, ecohydrological VRD model (††) per plant species and sampling site. b: mean rooting depth; Aro: cross-sectional area at the root collar.

	Site 1						Site 2						Site 3					
Plant species	*b* (mm)	$b^{\dagger}$ (mm)	$b^{\dagger\dagger}$ (mm)	*Aro* (mm^2)	$Aro^{\dagger}$ (mm^2)	$Aro^{\dagger\dagger}$ (mm^2)	*b* (mm)	$b^{\dagger}$ (mm)	$b^{\dagger\dagger}$ (mm)	*Aro* (mm^2)	$Aro^{\dagger}$ (mm^2)	$Aro^{\dagger\dagger}$ (mm^2)	*b* (mm)	$b^{\dagger}$ (mm)	$b^{\dagger\dagger}$ (mm)	*Aro* (mm^2)	$Aro^{\dagger}$ (mm^2)	$Aro^{\dagger\dagger}$ (mm^2)
E. minima	4.17±0.9	7.89	52.7	0.13±0.0	0.13	0.013	17.50±12.9	5.20	49.9	0.08±0.0	0.08	0.016	23.3±3.8	8.50	38.1	0.29±0.1	0.30	0.09
L. alpina	3.33±0.0	22.80	56.9	0.38±0.1	0.9	1.89	15.00±4.3	19.70	49.9	0.38±0.1	1.00	2.24	25.0±10	19.10	42.8	0.37±0.1	0.50	1.66
P. alpina	6.67±1.9	24.4	2.6	1.66±1.0	0.60	15.88	17.50±5.7	21.70	47.9	0.88±0.2	0.20	12.68	23.33±3.8	26.60	42.5	0.91±0.6	0.40	8.33

df=7 p=0.48; Aro:W=40 df=7 p=1 ;Table 4). The VRDs were different between plant species (χ^2:212.1 df:2 p<0.01) and they generally differed across study sites (χ^2:99.7 df:2 p<0.01). *L. alpina* had the widest and densest VRD followed by *P. alpina* and *E. minima* (Fig. 4; Table 4). However, the VRD for *P. alpina* tended to be deeper than for the other two plant species (Fig. 4; Table 4). A clear relationship between VRD and study site was not observed, indicating that the extent and depth of the VRD was not linked to the study site (Fig. 4).

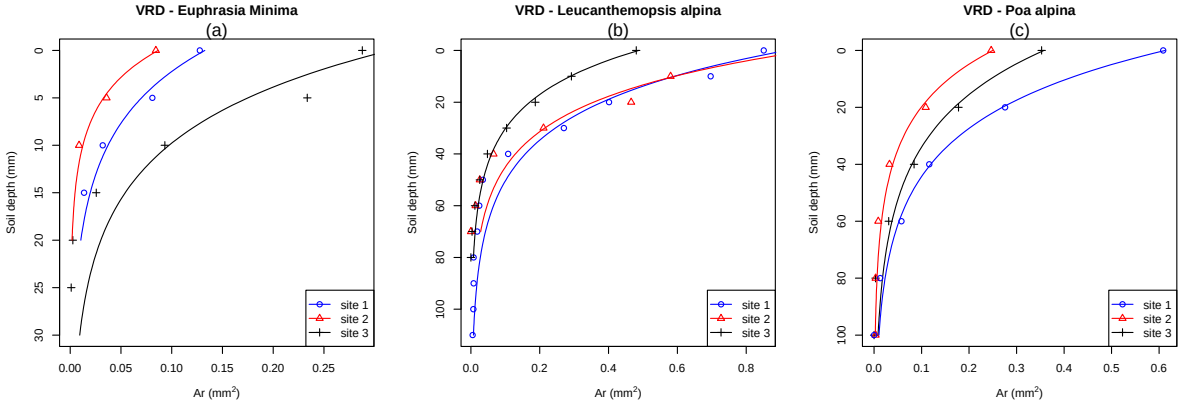

Figure 34. Vertical root distribution (VRD) for (a) Euphrasia minima, (b) Lecanthemopsis alpina, and (c) Poa alpina. Triangles, dots and crosses represent observed values for the root cross-sectional area of all roots found at a given soil depth as described in Section 2.4. The lines portray the nls exponential models fitted to the measured data points -i.e. empirical VRD model. See online version for colours.

3.5.Influence of plant and soil attributes on key vertical root distribution parameters

The cross-validation results from fitting random forest models to the key vertical root distribution (VRD) parameters (i.e. *b*, *Aro*, and *Mr*; Appendix A - Table A1 and Figure A1; Supplementary Material) suggested that the latter can be predicted successfully using the studied plant and soil attributes as predictors.

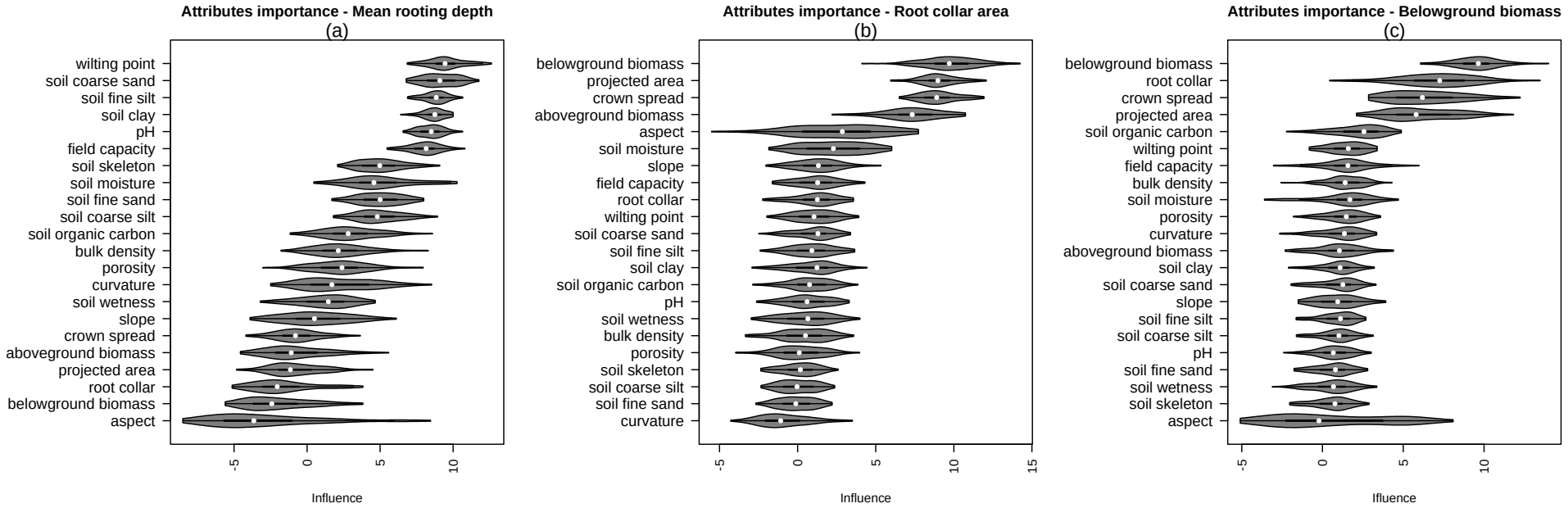

Figure 4~~5~~. Violin plots depicting the influence of the studied plant and soil attributes on relevant vertical root distribution (VRD) parameters -i.e. (a) mean rooting depth, b; (b) root collar area, Aro; (c) plant belowground biomass, Mr. The white dot within the violin plot boxes represent the median while the grey area around the box represents the probability density of the data at different values.

The mean rooting depth (*b*) was chiefly influenced by soil attributes (Fig. 5a) such as the soil volumetric moisture content at wilting point, followed by the soil texture (Fig. 5a). Soil pH and the soil moisture at field capacity also appeared to significantly influence *b* (Fig. 5a). In the light of the correlogram (Fig. 6), the rooting depth was strongly correlated to the soil texture, positively with clay and silt contents and negatively with coarse sand content. The slope aspect, the soil moisture, and organic carbon content also had a strong, positive correlation with *b* (Fig. 6). In the light of the PDPs (Appendix B - Fig. B1), there was a positive influence of the wilting point on *b* (i.e. the higher θwp the higher *b*), up to 3.4 %, after which a constant effect was observed. Field capacity also had a positive effect on *b* only detected when θfc was above 15.6 %. We noticed a negative influence of soil *pH* on *b* when the former was above 4.5. The attributes that did not have a substantial effect on *b* (Fig. 5a) had a remarkable effect when the PDPs were assessed (Appendix B - Fig. B1). For example, deeper root systems were found under steeper conditions. However, shallower root systems were encountered when soil was wetter, but shifts in the soil hydrological regime led to changes in the influence of soil moisture on *b*. A negative effect of soil moisture on *b* was observed under residual and saturated regimes, and a positive effect was noticed under the transitional regime. Contrariwise, soil porosity and organic carbon had a positive effect on *b* (Tables 2 and 3; Fig. 6) which was not detected in the PDPs for the soil porosity (Fig. B1).

The cross-sectional area at the root collar (*Aro*) was mostly affected by plant attributes (Fig. 5b). The root biomass, surface projected area, crown spread, and aboveground biomass had a significant influence on *Aro*. However, the investigated soil attributes did not have a substantial influence on *Aro* on the basis of the RF model outputs (Fig. 5b). In the light of the correlogram plot (Fig. 6), *Aro* had a strong, positive correlation with above- and belowground biomass but also with the soil water content at field capacity and wilting point. According to the PDPs

(Appendix B - Fig. B2), all the examined plant attributes had a consistent, positive effect on *Aro*. We also observed that some soil attributes had a consistent effect on *Aro* when the PDPs were examined (Fig. B2) that could not be detected in the correlogram (Fig. 6) or in relative influence plots (Fig. 5b). According to the PDPs, soil porosity, the percentage of clay, fine silt and fine sand had a negative effect on *Aro*, while the percentage of coarse sand and coarse silt had a positive effect. We also observed that *Aro* tended to be wider under steeper slope conditions, and narrower when soil organic carbon increased (Fig. B2).

The root biomass (*Mr*) was predominantly influenced by plant attributes (Fig. 5c) such as the aboveground biomass, *Aro*, crown spread, and plant's surface projected area. However, the influence of soil organic carbon on *Mr* was significantly higher than the influence of the rest of the studied soil attributes (Fig. 5c). In the light of the correlogram plot (Fig. 6), *Mr* had a strong, positive correlation with the aboveground biomass, the crown spread, and *Aro*. In addition, soil attributes, such as the soil moisture at field capacity and wilting point, also had a strong positive correlation, with the latter being the attribute with highest correlation to *Mr* (Fig. 6). According to the PDPs (Appendix B - Fig. B3), all the plant attributes studied had a consistent, positive effect on *Mr*. In addition, we noticed a consistent effect of some of the soil attributes studied on *Mr* which resembled the effects observed for *Aro* (Fig. B2).

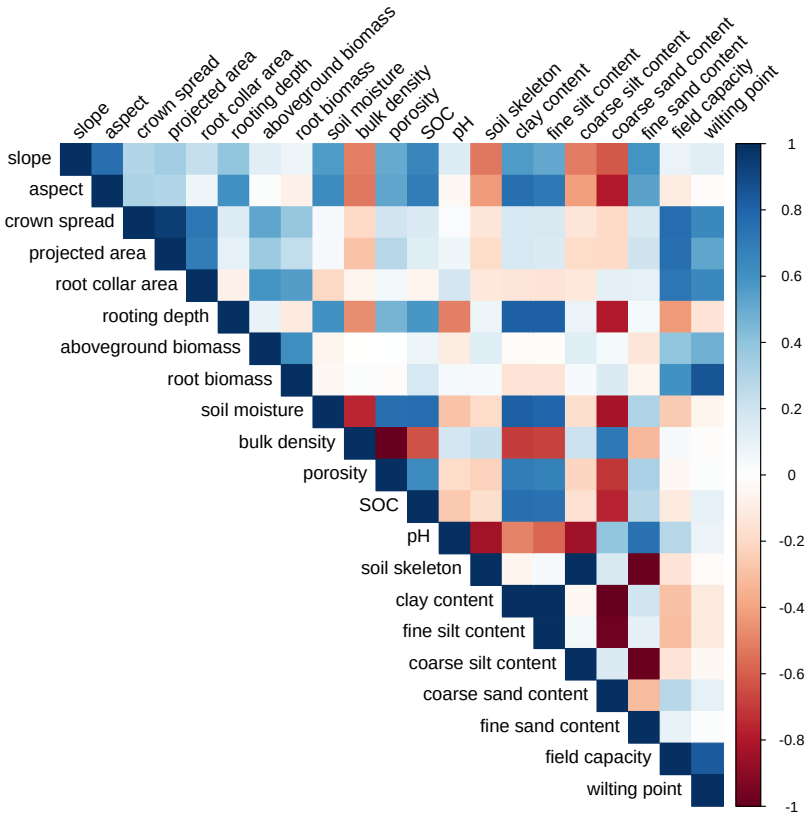

Figure ~~5~~6. Correlation plot depicting Pearson's correlation coefficient between the investigated plant and soil attributes. Blue colour: positive correlation; Red colour: negative correlation. The darker the colour shade, the higher the correlation between two attributes. See online version for colours.

3.6.Ecohydrological model for vertical root distribution

We found a substantial mismatch between the chosen parametric ecohydrological and the empirical VRD models (Figs. 8a-c; Table 4). This showed that the existing parametric, ecohydrological VRD model cannot readily predict VRD under the pedoclimatic conditions of the study area. However, we detected a consistent ($R^2 > 0.9$) linear relationship between the ecohydrological and empirical VRD models when *Ar(z)* was log-transformed (Figs. 8d-e) -i.e. a consistent exponential fit was observed when comparing empirical, untransformed *Ar(z)* values against parametric, untransformed *Ar(z)* values. The fitting parameters for the log-transformed linear models established between ecohydrological and empirical VRD models

are shown in Table 5. We observed a strong correlation ($r > 0.5$) between most of the studied plant attributes and the fitting parameters for the log-transformed linear models (Table 6). In addition, a strong correlation was observed between the fitting parameters and the soil moisture content at field capacity and at wilting point (Table 6).

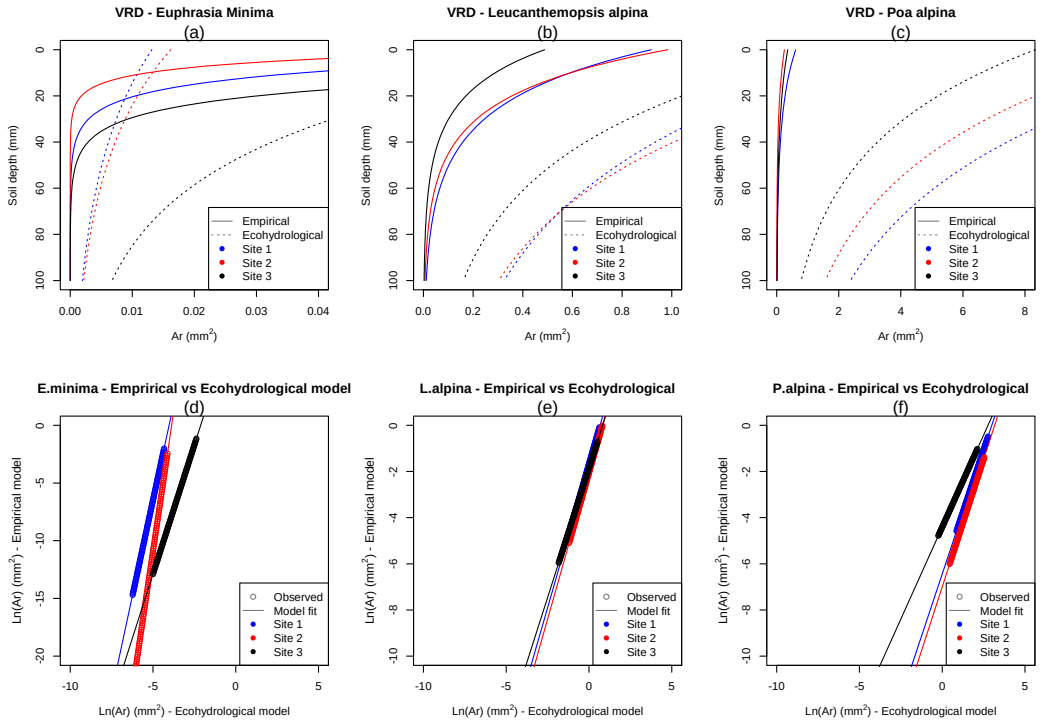

Figure ~~6~~7. (a-c) Vertical root distribution (VRD) models fitted with a nls exponential model to the measured data – i.e. empirical VRD model (solid lines) and with the parametric, ecohydrological VRD model (dotted line) (d-e) Mathematical relationship between empirical and ecohydrological VRD models established with a log-transformed linear model of the form "Ln(Empirical Ar(z))=A+BxLn(Ecohydrological Ar(z))" (see Table 5 for fitting parameters). Also, see online version of this manuscript for colours.

Table 35. Fitting parameters for the log-transformed linear model the form "Ln(Empirical Ar(z))=A+BxLn(Ecohydrological Ar(z))" fitted between empirical and ecohydrological VRD models.

	Site 1		Site 2		Site 3	
Plant species	A	B	A	B	A	B
E. minima	26.88	6.67	37.46	9.68	9.47	4.47
L. alpina	-1.67	2.49	-2.07	2.53	-1.86	2.24
P. alpina	-6.44	2.15	-7.00	2.21	-4.41	1.59

Table 46. Pearson's correlation coefficients for the pair-wise correlation between the evaluated soil and plant attributes and the fitting parameters for the log-transformed linear model the form "Ln(Empirical Ar(z))=A+BxLn(Eco-hydrological Ar(z))" fitted between empirical and ecohydrological VRD models.

Variable	A	B
Slope	-0.36	-0.42
Aspect	-0.31	-0.36
Curvature	-0.05	0.03
CS	-0.74	-0.73
Sp	-0.56	-0.58
Aro	-0.65	-0.60
Ma	-0.75	-0.68
Mr	-0.61	-0.54
b	-0.11	-0.11
θg	0.20	0.23
ρ_{bk}	-0.12	-0.14
n	0.18	0.20
SOC	-0.18	-0.20
pH	-0.12	-0.14
sk	-0.09	-0.16
Clay	0.19	0.29
Fine silt	-0.14	-0.16
Coarse silt	-0.12	-0.13
Fine sand	0.19	0.29
Coarse sand	-0.21	-0.31
θfc	0.16	0.19
θwp	-0.59	-0.57

549

550 4. Discussion

551 4.2.Vertical root distribution

552 The vertical root distribution (VRD) of the three studied alpine plant species decreased
553 exponentially with soil depth. Accordingly, VRD was successfully described with a negative
554 exponential model that was fitted to the measured data (Fig. 4). This is consistent with VRDs
555 reported for shrub, woody, and herbaceous plant species in Mediterranean (Preti et al., 2010;
556 Tron et al., 2014), southern alpine (Burylo et al., 2011) and temperate-humid ecosystems
557 (Gonzalez-Ollauri and Mickovski, 2016; Tardio et al., 2016), and it confirms that the proposed
558 approach for describing VRD in herbaceous plants is methodologically robust across terrestrial
559 ecosystems in Europe.

560

561 We attributed the observed VRD differences across plants and sites (Fig. 4) to the differences
562 in plant attributes that we found (Table 3). In spite of the differences observed in key VRD
563 parameters across sites (Table 3), and of the strong influence of site-specific attributes on the
564 key VRD parameters that we noticed herein (Fig. 5 and Section 4.2), the direction of the effect
565 of the study site on the size and depth of the measured VRDs was unclear, given that the extent
566 of VRD changed with the plant species from site to site (Fig. 4). Yet, there were limitations to
567 the study, as we did not evaluate altitudinal differences between plant individuals (e.g. Gale,
568 2004; Miyamoto et al., 2015), nor the differences in soil nutrients between sampling locations
569 (e.g. Forde and Lorenzo, 2001), or the climatic differences across study sites (Schenk and
570 Jackson, 2005). We think that all these aspects deserve further consideration to expand on our
571 findings related to how VRD is shaped by local site conditions.

572

573 The proposed VRD description approach has been used effectively in woody plant species
574 under both sloped and flat topographies (Tron et al., 2014; Tardio et al., 2016; Gonzalez-Ollauri
575 et al., 2020). Still, its ability to capture realistically large roots (> 3 mm in diameter, incl. tap
576 roots) in woody plants needs further verification, notwithstanding the fact that the *in situ*
577 description of root systems for woody plants is methodologically challenging (Böhm, 1979),
578 and it generally focuses on one or two vertical profiles of the root system (e.g. Tardio et al.,
579 2016; Gonzalez-Ollauri et al., 2020) from which it is hard to comprehensively capture root
580 system features. However, the VRD description approach followed herein is methodologically
581 simple and easy to implement, it provided a good and realistic picture of the VRD for the
582 studied alpine plants with root systems mainly comprising fine roots, and it generated
583 information directly applicable in workflows needing VRD information such as plant-water
584 uptake models (e.g. Laio, 2006; Shukla, 2014) or soil-root reinforcement estimation
585 approaches (e.g. Gonzalez-Ollauri and Mickovski, 2016, 2017b; Kokutse et al., 2016).
586
587 4.3.Influence of climate, plant and soil attributes on key vertical root distribution parameters
588
589 The rooting depth (*b*) and root biomass (*Mr*) for the three studied plant species (Table 3) were
590 within the ranges described in Pohl et al. (2011) and Hudek et al. (2017) for alpine ecosystems.
591 However, these were below the ranges reported for semi-arid (Preti et al., 2010) and temperate-
592 humid (Gonzalez-Ollauri and Mickovski, 2016) climates. These differences were attributed to
593 the short duration of the growing season in our study area, and associated to long periods with
594 snow cover and low temperatures, which likely limited plant development (e.g. Kaspar and
595 Bland, 1992; Lahti et al., 2005; Alvarez-Uria and Körner, 2007).
596

The key studied VRD parameters (i.e. *b*: mean rooting depth; *Aro*: cross-sectional area at the root collar; and *Mr*: root biomass) were distinctly influenced by the investigated soil and plant attributes (Figs 6, 7 and Appendix B – Figs. B1-B3). We observed that, while the rooting depth was mostly site-specific, the allocation of biomass to the belowground plant parts and its distribution along the soil profile was both species-specific and reliant on relevant soil ecohydrological features.

4.3.1. Rooting depth

The mean rooting depth (*b*; Laio et al., 2006) was chiefly influenced by soil attributes governing the water available to plants in the soil (WAP; i.e. difference between soil water content at field capacity (θfc) and wilting point (θwp); Fig. 5a, 7 and Appendix B – Fig. B1; Table 4; Eq.4 Table 1; Casper et al., 2003). It is worth noting that θfc and θwp were estimated in the light of well-established pedotransfer functions nested in the VRD model (Eqs. 4, 5, 11 and 12; Table 1) with relatively low sensitivity (Gonzalez-Ollauri and Mickovski, 2016) and which employed soil texture, soil organic carbon, and porosity as inputs (Toth et al., 2015). Accordingly, soils with high organic carbon and with a fine texture (i.e. high clay and silt content) would have high water retention capacity (Kirkham, 2005; Lu and Likos, 2004) and, as a result, deeper root systems, as it was shown herein (Figs. 6 and B1; Table 3; Schenk and Jackson, 2005; Gonzalez-Ollauri and Mickovski, 2016). In fact, we observed clear differences across sites in terms of the soil attributes governing WAP (Table 2), which may explain why Site 3 had substantially deeper rooting depths than sites 1 and 2 (Table 3). The effect of the soil's ecohydrological characteristics on the rooting depth has been highlighted in previous studies (e.g. Schenk, 2005; Laio et al., 2006; Preti et al., 2010), suggesting that the ability of roots to explore the soil in depth largely depends on the water mass balance within the topsoil

(Tsutsumi et al., 2003; Laio, 2006; Laio et al., 2006). In fact, the soil water mass balance features in the proposed ecohydrological models predicting the mean rooting depth (Eqs. 4 and 5; Table 1; Laio et al., 2006; Gonzalez-Ollauri and Mickovski, 2016), and our results validate that these models are conceptually correct. However, other models are nested into the investigated VRD model (e.g. growing season duration, evapotranspiration, soil pedotransfer functions, etc.), leading to likely propagation of errors and uncertainty (Taylor, 1997) that should be thoroughly investigated and dealt with prior to verifying the quality and robustness of the VRD models (e.g. Gonzalez-Ollauri and Mickovski, 2017b).

Model differences between the options for arid or semi-arid (Eq. 4; Table 1) and temperate humid (Eq.5; Table 1) climates imply rooting depth differences that were not tested herein. In arid climates, water withdrawal through evapotranspiration limits the amount of water available to plants in the topsoil, thus encouraging deeper rooting depths than in humid climates. By contrast, in temperate humid climates, water inputs exceed outputs in the topsoil (i.e. rainfall > evapotranspiration), leading to shallower rooting depths as roots do not face water limitations in the topsoil - i.e. roots do not need to explore the soil in search of deep water (Schenk and Jackson, 2005). In alpine climates, however, where snowfall, ground frost, and short snow-free periods govern the soil ecohydrological behaviour (e.g. Molotch et al., 2009), further model tuning is needed to fully capture the rooting depth and VRD with the proposed parametric ecohydrological model (Fig. 7a-c; Table 4). In addition, the direct quantification of soil attributes governing the available water to plants through, for example, retrieving the soil-water retention function (e.g. Zhang et al., 2019) or by evaluating the soil structure and aggregates (e.g. Bengough, 2003) could shed more light on the effect of the soil's ecohydrological characteristics on the rooting depth and VRD.

It is also worth noting the high influence of soil pH on the rooting depth (Fig. 4a; Fig. 6), which on the basis of the correlogram (Fig. 6) and PDPs (Annex B – Fig.B1) was negative – i.e. shallower rooting depths were noticed when the pH was higher. This observation may indicate that plants tend to reduce root elongation and increase thickness as a strategy to promote nutrient uptake when soil pH is high (e.g. Robles-Aguilar et al., 2019). The latter is somehow supported by the positive interaction that we observed between soil pH and the cross-sectional area at the root collar (*Aro*; Figs. 6 and B2), suggesting that root thickness increased at the collar when soil pH increased. Yet, as the variability in soil pH was small across study sites (Table 3), we cannot convincingly elucidate possible reasons behind our observations and we thus recommend further research on the effect of soil pH on the key VRD parameters.

In this study, there were also limitations to the analysis because site-specific records for the climate attributes and for the snowpack depth, although capable of affecting the rooting depth in alpine ecosystems (e.g. Cooper et al., 2011), were not available. Additionally, we did not consider the topographical effect of the slope gradient on the rainfall lost to runoff and, in turn, on the rooting depth (Tron et al., 2014; Tardio et al., 2016); nor the influence of preferential flow paths in the soil (e.g. Clothier et al., 2008; Gonzalez-Ollauri et al., 2020) or the effect of soil anisotropy on the rooting depth and VRD. We believe that all these aspects deserve detailed consideration to improve the predictive capacity of the parametric VRD models studied here. However, the consistent linear relationship between empirical and parametric ecohydrological VRD models reported in this study (Fig. 7d-e), and the high correlation found between fitting parameters and soil attributes governing the available water to plants (i.e. θfc and θwp; Table 6) set the direction of future research.

4.3.2. Cross-sectional area at the root collar and root biomass

The cross-sectional area at the root collar (*Aro*) and the root biomass (*Mr*) were mostly influenced by the investigated plant attributes (Fig. 5 and Appendix B – Figs. B2 and B3). However, a substantial effect of the soil water at field capacity and wilting point on *Aro* and *Mr* was also detected (Fig. 6). It is worth noting that the combined effect of the soil and plant attributes on the key VRD parameters was only evident when multiple data analysis approaches were used together - i.e. relative influence from RF models (Fig. 5), pairwise correlation (Fig. 6) and PDPs (Appendix B), indicating that comprehensive data mining is needed to fully grasp complex interactions between environmental variables affecting VRD (Supplementary Material - Fig. S1). The findings shown herein corroborate that while the extent of the root system in the soil (i.e. rooting depth; Section 4.2.1) is delimited by the soil water mass balance and its contributing soil attributes (i.e. soil texture, *SOC*, θfc and θwp; Figs. 5a and 6), the plant biomass allocated belowground is distributed along the VRD profile in the light of both plant-specific and soil attributes (Figs. 6b-c and 7). The latter aspect features in the proposed VRD model through *Aro* (Eq.3; Table 1), which acts as scaling factor in the distribution of root biomass along the root profile in the soil (Preti et al., 2010; Gonzalez-Ollauri and Mickovski, 2016). In this regard, we noticed that the magnitude of *Aro* was positively influenced by the slope gradient whilst being negatively affected by SOC (Fig. B2). A plausible explanation for the former is that plants tend to adopt anchoring strategies in steep slopes (e.g. Tardio et al., 2016), which may imply the allocation of root biomass near the ground surface to promote anchorage to the ground and plant stability (Chiatante et al., 2003). In fact, we also noticed that *Mr* was higher on steeper slopes (Fig. B3). Contrariwise, root biomass tends to be distributed towards deeper portions of the soil when there is more SOC, which would reduce the amount of root biomass allocated near the surface (Fig. B3) and thus to *Aro*. All these aspects support the assumption of using a 'cone-shape-volume' to model the distribution of root biomass in the

soil (Fig. 3b; Supplementary Material), which was further supported by the strong influence of *Mr* on *Aro* (Figs.6b and 7). However, the observed mismatch between empirical and parametric ecohydrological VRD models (Fig. 7a-c; Table 4), in which *Aro*, *Mr*, and *b* are embedded (Table 1), suggests that the modelling approach to estimate the key VRD parameters *Aro* and *b* (Eqs. 4, 5 and 7; Table 1) must be revised for alpine ecosystems. Future work may consider to explore the effect of topography in detail and/or to include climate-specific variables such as snowpack depth, duration of the snow-free period, and frozen ground cycle, and how these influence *AWP* and *Aro* in alpine ecosystems. In addition, soil nutrient limitations (e.g. nitrogen; Zong et al., 2020) and plant-specific aspects related to growth and survival strategies of alpine plants (e.g. Cooper et al., 2003; Germino, 2014) can be considered in future versions of the VRD model to portray more realistically the characteristic allocation of plant biomass above- and belowground in alpine ecosystems (e.g. Wu et al., 2013).

Nonetheless, the strong correlation between the investigated plant attributes and the fitting parameters resulting from evaluating the relationship between empirical and parametric, ecohydrological VRD models (Table 6) suggests that the collection of studied plant attributes was appropriate, setting the direction of future research. The strong influence of plant attributes such as the crown spread and projected area on the plant aboveground biomass (*Ma*) and *Aro* (Figs.6b-c, 7, Appendix B – Figs. B2 and B3) hints at the possibility of establishing robust data-mining approaches able to predict VRD on the basis of easy-to-measure aboveground plant attributes (e.g. Fig. 3); provided that information on the allometry relationship between above and belowground plant parts is available (Table 2; e.g. Cheng and Niklas, 2007). In this regard, we expected that the allometry ratio (i.e. *ALR=Mr/Ma*; Table 2) would be consistently above unity in the studied alpine plant species (e.g. Pohl et al., 2011), as a greater allocation of biomass to the belowground plant parts could help plants to withstand harsh aboveground

conditions (Germino, 2014). Nonetheless, only *P. alpina* had an *ALR* consistently above unity. Future work helping to establish consistent and site-specific allometry relationships between above and belowground plant parts in alpine ecosystems (e.g. Šťastná et al. 2012) will undoubtedly help to consolidate approaches seeking to describe VRD using very few, easily measurable, parameters, like the one discussed herein.

5. Conclusion

Our study consolidates a simple protocol to describe the vertical root distribution (VRD) in herbaceous plants. It also addresses, for the first time, the influence of soil and plant attributes on key VRD parameters, validating the principles and assumptions behind the existing parametric, ecohydrological models predicting VRD, and casting light on how VRD can be effectively described using simple climate, soil and plant attributes. In fact, we confirmed that insights into the water mass balance in the soil and into the water available to plants are crucial to describe VRD in alpine ecosystems, as it has been suggested in previous studies for semi-arid and temperate humid ecosystems. However, the existing parametric ecohydrological VRD models were not able to portray successfully the vertical root distribution of the studied alpine plants in the light of the measured root profiles. Although we found a strong correlation between empirical and parametric VRD models that establish a clear direction for future research, we also think that the parametric VRD model needs to be revised in the future to include features affecting the water available to plants in alpine ecosystems, such as the snowpack characteristics or the length of the snow-free and frozen ground periods. We also encourage future work exploring in detail the effect of topography, elevation, climate and nutrient limitations on VRD, as these factors can help to formulate new models predicting VRD realistically.

CRediT authorship contribution statement

Alejandro Gonzalez-Ollauri: funding acquisition, conceptualization, methodology, data curation, formal analysis, investigation, project administration, writing - original draft, writing – review & editing

Csilla Hudek: investigation, writing – review & editing

Slododan B. Mickovski: funding acquisition, methodology, project administration, writing – review & editing

Davide Viglietti: investigation

Nicole Ceretto: investigation

Michele Freppaz: project administration, resources, writing – review & editing

Acknowledgement

We acknowledge the useful comments and suggestions from three anonymous referees and the Editor that helped us to improve the manuscript. The contribution of A. Gonzalez-Ollauri and S.B. Mickovski was funded by Erasmus+ project ECOMED (575796-EPP-1-2016-ES-EPPKA2-KA) and the Green4Brown Project (M315-10363) funded by the BEAM Research Centre of the Glasgow Caledonian University.

6. References

Alvarez-Uria, P., Körner, C., 2007. Low temperature limits of root growth in decidious and evergreen temperate tree species. Funct. Ecol. 21, 211–218.

771 Arnone, E., Caracciolo, D., Noto, L. V., Preti, F., and Bras, R. L., 2016. Modeling the
772 hydrological and mechanical effect of roots on shallow landslides, *Water Resour*.
773 *Res.*, 52, 8590– 8612, doi:10.1002/2015WR018227.

774 ASTM (1995) D 4972-95a: Standard test method for pH of soils. ASTM International, West
775 Conshohocken, PA, USA.

776 Asturnauta, 2020. *Euphrasia minima*. https://www.asturnatura.com/especie/euphrasia-
777 minima.html. Retrieved on 07/07/2020.
778 Bengough A.G. (2003) Root Growth and Function in Relation to Soil Structure,
779 Composition, and Strength. In: de Kroon H., Visser E.J.W. (eds) Root Ecology.
780 Ecological Studies (Analysis and Synthesis), vol 168. Springer, Berlin, Heidelberg.
781 https://doi.org/10.1007/978-3-662-09784-7_6

782 Blozan, W., 2008. Tree measuring guidelines of the eastern native tree society. Bull. East.

783 Native Tree Soc. 1 (1), 3–10.

784 Böhm, W., 1979. Methods of Studying Root Systems. Springer Verlag, Berlin.

785 Breiman, L., 2001. Random forests. Mach. Learn. 45, 5–32.

786 Burylo, M., Hudek, C., Rey, F., 2011. Soil reinforcement by the roots of six dominant species
787 on eroded mountainous marly slopes (Southern Alps, France). Catena, 84: 70-78.
788 Burylo, M., Dutoit, T. and Rey, F., 2014. Species Traits as Practical Tools for Ecological
789 Restoration of Marly Eroded Lands. Restor Ecol, 22: 633-640. doi:10.1111/rec.12113

790 Casper, B.B., Schenk, H.J., Jackson, R.B., 2003. Defining a Plant's Belowground Zone of
791 Influence. Ecology 84 (9), 2313–2321.

792 Cheng, D., Niklas, K.J., 2007. Above- and below-ground biomass relationships across 1534
793 forested communities. Ann. Bot. 99, 95–102.

794 Chiatante, D., Scippa, S.G., Di Lorio, A., Sarnataro, M., 2003. The influence of steep slopes
795 on root system development. J. Plant Growth Regul. 21, 247–260.

796 Clothier, B.E., Green, S.R. and Deurer, M., 2008. Preferential flow and transport in soil:
797 progress and prognosis. European Journal of Soil Science, 59: 2-13. doi:10.1111/j.1365-
798 2389.2007.00991.x
799 Cooper, E., Dullinger, S., Semenchuk, P., 2011. Late snowmelt delays plant development and
800 results in lower reproductive success in the High Arctic. Plant science, 180:157-67.
801 10.1016/j.plantsci.2010.09.005.
802 Coutts, M.P., Nielsen, C.C.N., Nicoll, B.C., 1999. The development of symmetry, rigidity and
803 anchorage in the structural root system of conifers. Plant and Soil 217, 1-15.

804 Darwin, C., 1880. The Power of Movement in Plants. John Murray, London, UK.

805 Fitter, A.H., Stickland, T.R., 1991. Architectural analysis of plant root systems 2. Influence of
806 nutrient supply on architecture in contrasting plant species. New phytologist, 118: 383-
807 389.
808 Forde, B., Lorenzo, H., 2001.The nutritional control of root development. Plant and
809 Soil, **232:** 51–68. https://doi.org/10.1023/A:1010329902165
810 Freppaz, M., Filippa, G., Caimi, A., et al., 2010. Soil and plant characteristics in the alpine
811 tundra (NW Italy). In: Tundras: Vegetation, Wildlife and Climate Trends. Nova Publishers.
812 pp 81–110.

813 Freppaz, M., Viglietti, D., Balestrini, R., Lonati, M., Colombo, N., 2019. Climatic and
814 pedoclimatic factors driving C and N dynamics in soil and surface water in the alpine tundra
815 (NW-Italian Alps). Nature Conservation, 34: 67-90.
816 Fuller, W. A. 1987. Measurement Error Models. John Wiley & Sons. ISBN 978-0-471-86187-
817 4.
818 Gale J. (2004). Plants and altitude--revisited. Annals of botany, 94(2), 199.
819 https://doi.org/10.1093/aob/mch143
820 Germino M.J. 2014. Plants in Alpine Environments. In: Monson R. (eds) Ecology and the
821 Environment. Springer, New York, NY
822 Goodman, A.M., Ennos, A.R., 1999. The Effects of Soil Bulk Density on the Morphology and
823 Anchorage Mechanics of the Root Systems of Sunfower and Maize. Annals of Botany, 83:
824 293-302.

825 Gonzalez-Ollauri, A., Mickovski, S.B., 2016. Using the root spread information of pioneer
826 plants to quantify their mitigation potential against shallow landslides and erosion. Ecol. Eng.
827 95, 302–315.

828 Gonzalez-Ollauri, A., Mickovski, S.B., 2017a. Plant-soil reinforcement response under
829 different soil hydrological regimes. Geoderma 285, 141–150.

830 Gonzalez-Ollauri, A. and Mickovski, S.B., 2017b. Plant-Best: A novel plant selection tool for
831 slope protection. Ecological Engineering 106 (2017) 154–173
832 Gonzalez-Ollauri, A. and Mickovski, S.B., 2017c. Shallow landslides as drivers for slope
833 ecosystems evolution and biophysical diversity. Landslides, 14(5), 1699-1714. DOI
834 10.1007/s10346-017-0822-y
835 Gonzalez-Ollauri, A., Mickovski, S.B., 2018. Green for Brown (G4B): A Novel Tool for
836 Evaluating Phytoextraction in Soils Polluted by Heavy Metals. In: Kallel A., Ksibi M., Ben

837 Dhia H., Khélifi N. (eds) Recent Advances in Environmental Science from the Euro-
838 Mediterranean and Surrounding Regions. EMCEI 2017. Advances in Science, Technology &
839 Innovation (IEREK Interdisciplinary Series for Sustainable Development). Springer, Cham.
840 http://doi-org-443.webvpn.fjmu.edu.cn/10.1007/978-3-319-70548-4_81
841 Gonzalez-Ollauri, A., Stokes, A., Mickovski, S.B., 2020. A novel framework to study the effect
842 of tree architecture in stemflow yield and its consequences for soil-water dynamics. Journal of
843 Hydrology, 582: 124448.

844 Greenwell, B.M., 2017. pdp: An R package for constructing partial dependence plots. R J. 9
845 (1), 421–436.

846 Greve, P., Roderick, M.L., Ukkola, A.M., Wada, Y., 2019. The aridity index under global
847 warming. Environ. Res. Lett., 14: 124006.
848 Hastie, T., Tibshirani, R., Friedman, J., 2009. The Elements of Statistical Learning, Second
849 Edition, Section 10.13.2, Springer, 2009.

850 Head, K.H., 1980. Manual of Soil Laboratory Testing. CRC Press, Boca Raton,US.

851 Herbert, D.A., Rastetter, E.B., Gough, L., Shaver, G.R.., 2004. Species diversity across
852 nutrient gradients: an analysis of resource competition in model ecosystems. Ecosystems
853 7:296–310

854 Hudek, C., Stanchi, S., D'Amico, M., Freppaz, M., 2017a. Quanitfying the contribution of the
855 root system of alpine vegetation in the soil aggregate stability of moraine. International Soil
856 and Water Conservation Research, 5: 36-42.
857 Hudek, C., Sturrock, C.J., Atkinson, B.S., Stanchi, S., Freppaz, M., 2017b. Root morphology
858 and biomechanical characteristics of high-altitude alpine plant species and their potential in
859 soil stabilization. Ecological Engineering, 109, Part B: 228-239.

Iversen, C. M., Sloan, V.L., Sullivan, P.F., Euskirchen, E.S., McGuire, A.D., Norby, R.J., Walker, A.P., Warren, J.M., Wullschleger, S.D., 2014. The unseen iceberg: plant roots in arctic tundra. New Phytologist, 205: 34-58.

Jackson, R.B., Canadell, J., Ehleringer, J.R., Mooney, H.A., Sala, O.E., Schulze, E.D., 1996. A global analysis of root distributions for terrestial biomes. Oecologia 108, 389–411.

Jarvis, N., 1989. A simple empirical model of root water uptake. Journal of Hydrology, 107:57-72.

Kaspar, T.C., Bland, W. L., 1992. Soil temperature and root growth. Soil Science, 154(4):290-299.

Kirkham, M. B., 2005. Principles of Soil and Water Retentions. Elsevier, Amsterdam, NL.

Kleidon, A., 2004. Global datasets of rooting zone depth inferred from inverse methods, J. Clim., 17(13), 2714– 2722.

Kokutse, N. K., Tranquille Temgoua, A. G., Kavazović,Z., 2016. Slope stability and vegetation: Conceptual and numerical investigation of mechanical effects. Ecological Engineering, 86:146-153, https://doi.org/10.1016/j.ecoleng.2015.11.005.

Köppen, W., 1884. The thermal zones of the Earth according to the duration of hot, moderate amd cold periods and the impact of heat on the organic world. Meteorol. Z. 1, 215–226.

Köstler, J. N., Bru¨ckner, E., et Bibelriether, H. 1968: Die Wurzeln der Waldbau¨me edn. Verlag Paul Parey.

Kuhn, M. et al., 2018. caret: Classification and Regression Training. R package version 6. 0.81. https://CRAN.R-project.org/package=caret.

881 Kutschera L., Lichtenegger E., 1992. Wurzelatlas mitteleuropaischer Griinlandpflanzen. Band
882 2: Pteridophyta und Dicotyledoneae; Teil 1: Morphologie, Anatomie, Okologie, Verbreitung,
883 Soziologie, Wirtschaft. Gustav Fischer, Stuttgart
884 Laio, F., 2006. A vertically extended stochastic model of soil moisture in the root zone. Water
885 Resources Research, 42:W02406
886 Laio, F., D'Odorico, P., Ridolfi, L., 2006. An analytical model to relate the vertical root
887 distribution to climate and soil properties. Geophys. Res. Lett., 33 (2006), p. L18401
888 Lahti, M., Aphalo, P., Finér, L., Ryyppö, A, Lehto, T., Mannerkoski, H., 2005. Effects of soil
889 temperature on shoot and root growth and nutrient uptake of 5-year-old Norway spruce
890 seedlings. Tree physiology, 25: 115-22. 10.1093/treephys/25.1.115.
891 Liaw, A., Wiener, M., 2002. Classification and Regression by randomForest. R News 2(3):
892 18-22.

893 Lu, N., Likos, W.J., 2004. Unsaturated Soil Mechanics. John Wiley and Sons, Hoboken,

894 US.

895 Lucherini, A., Gonzalez-Ollauri, A., Mickovski, S.B., 2020. The effect of vegetation on soil
896 polluted with galligu: phytostabilisation and novel approaches to evaluate soil galligu
897 concentration. Environmental Geotechnics, https://doi.org/10.1680/jenge.19.00031
898 Lynch, J., 1995. Root architecture and plant productivity. Plant Physiol. 109:7-13.
899 Matthies, D. 1998. Influence of the host on growth and biomass allocation in the two facultative
900 root hemiparasites Odontites vulgaris and Euphrasia minima. Flora (1998) 193, 187-193

901 McMaster, G.S., Wilhelm, W.W., 1997. Growing degree-days: one equation, two
902 interpretations. Agric. Forest Meteorol. 87, 291–300.

903 Mickovski, S.B., van Beek, L.P.H. & Salin, F. Uprooting of Vetiver Uprooting Resistance of
904 Vetiver Grass (Vetiveria zizanioides). Plant Soil 278, 33–41 (2005).
905 Miyamoto, K., Wagai, R., Aiba, S. *et al.* Variation in the aboveground stand structure and
906 fine-root biomass of Bornean heath (kerangas) forests in relation to altitude and soil nitrogen
907 availability. *Trees* **30,** 385–394 (2016). https://doi.org/10.1007/s00468-015-1210-7
908 Molotch, N.P., Brooks, P.D., Burns, S.P., Litvak, M., Monson, R.K., McConnell, J.R. and
909 Musselman, K. (2009), Ecohydrological controls on snowmelt partitioning in mixed-conifer
910 sub-alpine forests. Ecohydrol., 2: 129-142. doi:10.1002/eco.48
911 Pierce, S., Stirling, C. M., Baxter, R., 2000. Architectural and physiological heterogeneity
912 within the synflorescence of the pseudoviviparous grass *Poa alpina* var. vivipara L. Journal of
913 Experimental Botany, 51(351):1705-1712.
914 Pohl, M., Stroude, R., Buttler, A., Rixen, C., 2011. Functional trails and root morphology of
915 alpine plants. Annals of Botany, 108: 537-545.

916 Preti, F., Giadrossich, F., 2009. Root reinforcement and slope bioengineering sta- bilization
917 by Spanish Broom (Spartium junceum L.). Hydrol. Earth Syst. Sci. 13, 1713–1726.

918 Preti, F., Dani, A., Laio, F., 2010. Root profile assessment by means of hydrological,
919 pedological and above-ground vegetation information for bio-engineering purposes.
920 Ecological Engineering, 36:305-316.
921 Preti, F., 2013. Forest protection and protection forest: Tree root degradation over hydrological
922 shallow landslides triggering. Ecological Engineering, 61P:633-645.

923 Priestley, C., Taylor, R., 1972. On the assessment of surface heat flux and evaporation using
924 large-Scale parameters. Mon. Weather Rev. 100 (2), 81–92.

925 Quine, C.P., Burnand, A.C., Coutts, M.P., Reynard, B.R., 1991. Effects of mounds and

926 stumps on the root architecture of Sitka spruce on a peaty gley restocking site. Forestry 64,
927 385-401.

928 R Core Team, 2018. R: A Language and Environment for Statistical Computing. R
929 Foundation for Statistical Computing, Vienna, Austria https://www.R-project.org/.

930 Rodríguez-Iturbe, I., & Porporato, A., 2005. Ecohydrology of Water-Controlled Ecosystems:
931 Soil Moisture and Plant Dynamics. Cambridge: Cambridge University Press.
932 doi:10.1017/CBO9780511535727

933 Schenk, H.J., Jackson, R.B., 2005. Mapping the global distribution of deep roots in relation to
934 climate and soil characteristics. Geoderma 126, 129–140.

935 Schenk, H., 2005. Vertical vegetation structure below ground: scaling from root to globe.
936 Progr. Bot. 66, 341–373.

937 Shukla M. (2014) Soil Physics: An Introduction. Boca Raton, Florida: CRC Press.

938 Šťastná, P., Klimešová, J., Doležal, J., 2012. Altitudinal changes in the growth and allometry
939 of *Rumex alpinus* . *Alp Botany* **122,** 35–44. https://doi.org/10.1007/s00035-012-0099-7
940

941 Stokes, A., Atger, C., Bengough, A.G., Fourcaud, T., Sidle, R.C., 2009. Desirable plant root
942 traits for protecting natural and engineered slopes against landslides. Plant and Soil 324 (1), 1–
943 30.
944 Strobl, C., Boulesteix, A., Kneib, T. *et al.*, 2008. Conditional variable importance for random
945 forests. BMC Bioinformatics 9**,** 307. https://doi.org/10.1186/1471-2105-9-307

946 Tardio, G., Gonzalez-Ollauri, A., Mickovski, S.B., 2016. A non-invasive root distribution
947 analysis methodology from a slope stability approach. Ecol. Eng. 97, 46–57.

948 Taub, D.R., Goldberg, D., 1996. Root system topology of plants form habitats differing in soil
949 resource availability. Functional Ecology 10, 258-264.
950 Taylor, J. R., 1997. An introduction to error analysis: The study of uncertainties physical
951 measurements (2nd Edition). University Science Books, CA, USA.

952 Toth, B., Weynants, M., Nemes, A., Mako, A., Bilas, G., Toth, G., 2015. New generation of
953 hydraulic pedotransfer functions for Europe. Eur. J. Soil Sci. 66, 226–238.

954 Tron, S., Dani, A., Laio, F., Preti, F., Ridolfi, L., 2014. Mean root depth estimation at
955 landslide slopes. Ecol. Engine 69, 118–125.

956 Tsutsumi, D., Kosugi, K., Mizuyama, T., 2003. Effect of hydrotropism on root system
957 development in soybean (Glycine max): growth experiments and model simulation. J. Plant
958 Growth Regul. 21, 441–458.

959 Ukwildflowers (2020). *Lucanthemopsis alpina*.
960 https://www.ukwildflowers.com/Web_pages/leucanthemopsis_alpina_alpine_moon_daisy.ht
961 m). Retrieved on 07/07/2020.
962 van Wijk, M. T., and Bouten, W., 2001). Towards understanding tree root profiles: Simulating
963 hydrologically optimal strategies for root distribution, Hydrol. Earth Syst. Sci., 5(4), 629– 644.
964 Verma, P, George, KV, Singh, HV, Singh, SK, Juwarkar, A, Singh, RN, 2006. Modeling
965 rhizofiltration: heavy-metal uptake by plant roots. Environmental Modeling and Assessment,
966 11, 387-394.
967 Waisel, Y., Eshel, A., Kafkafi. U., (Eds.) 2002. Plant Roots: The Hidden Half, Marcel Dekker,
968 New York.

969 Wu, J., Shen, Z., Zhang, X. et al. Biomass allocation patterns of alpine grassland species and
970 functional groups along a precipitation gradient on the Northern Tibetan Plateau. J. Mt. Sci.
971 10, 1097–1108 (2013). https://doi.org/10.1007/s11629-013-2435-9
972 Zeng, X. 2001. Global Vegetation Root Distribution for Land Modeling. Journal of
973 Hydrometeorology, 2 (2001): 525-530.
974 Zhang J, Wang J, Chen J, Song H, Li S, Zhao Y, Tao J and Liu J (2019) Soil Moisture
975 Determines Horizontal and Vertical Root Extension in the Perennial Grass Lolium perenne L.
976 Growing in Karst Soil. Front. Plant Sci. 10:629. doi: 10.3389/fpls.2019.00629
977 Zong, N, Song, M, Zhao, G, Shi, P., 2020. Nitrogen economy of alpine plants on the north
978 Tibetan Plateau: Nitrogen conservation by resorption rather than open sources through
979 biological symbiotic fixation. Ecol Evol. 2020; 10: 2051– 2061.
980 https://doi.org/10.1002/ece3.6038
981 Zuo, C., and R. Zhang (2002), Estimating root-water-uptake using and inverse method, Soil
982 Sci., 167(9), 561– 571.
983

Appendix A: Goodness of fit of the Random Forest models fitted to key vertical root distribution parameters

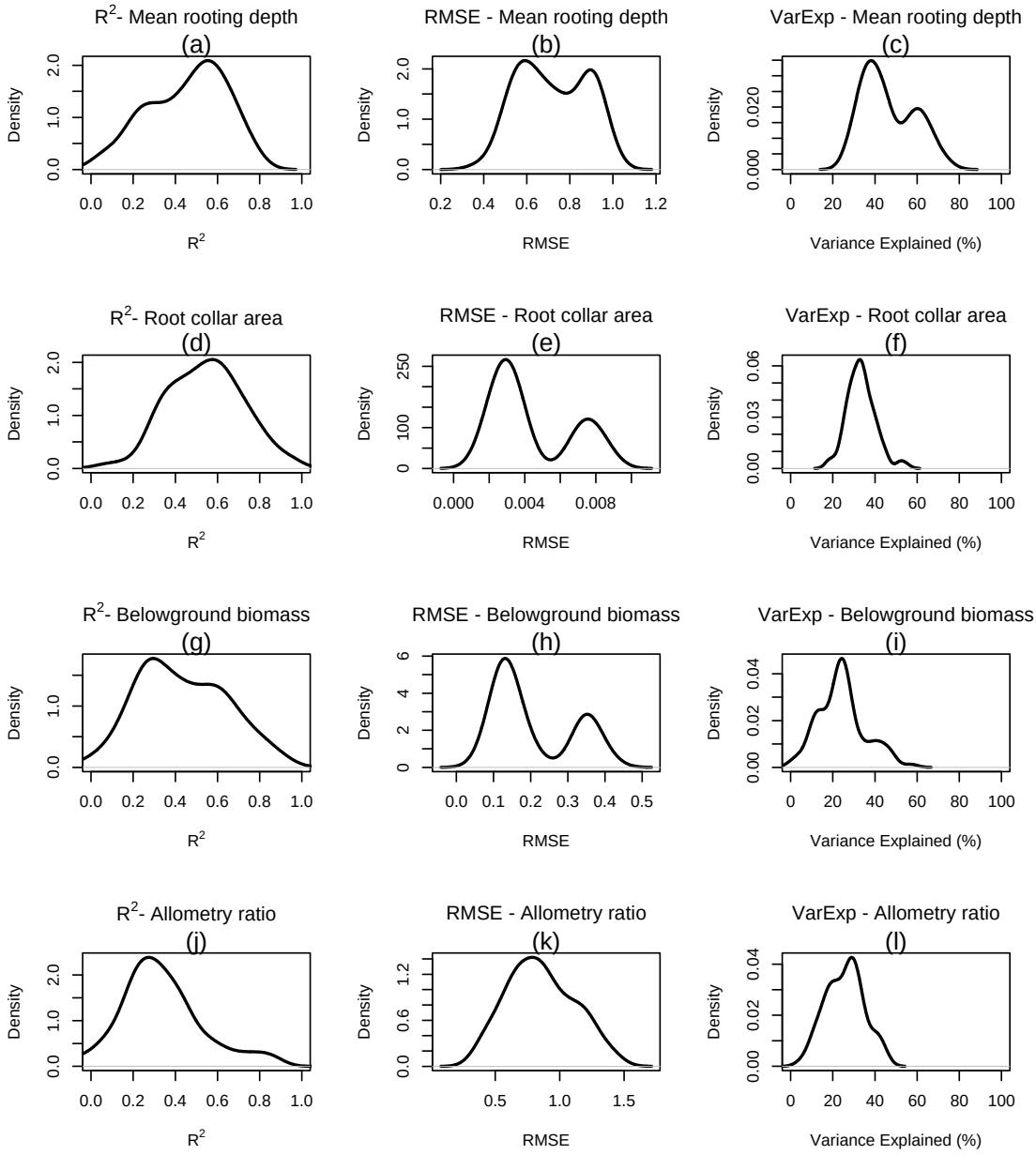

Figure A1. Probability density functions illustrating the coefficients of determination (R^2), root mean square error (RMSE) and variance explained (VarExp) retrieved from the cross-validation process implemented on random forest (RF) models, fitted between the studied soil and plant attributes to predict key vertical root distribution parameters.

994 *Table A1. Coefficient of determination (R^2) and root mean square error (RMSE) for the best performing random forest*
995 *models fitted between the key vertical root distribution (VRD) parameters mean rooting depth (b), cross-sectional area at*
996 *the root collar (Aro) and root biomass (Mr) and the studied plant and soil attributes.*

	R^2	RMSE	Model No.
b	0.78	0.67	28
Aro	0.92	0.003	78
Mr	0.90	0.11	68

997

998

Appendix B: Partial dependence plots (PDPs) for the key vertical root distribution parameters

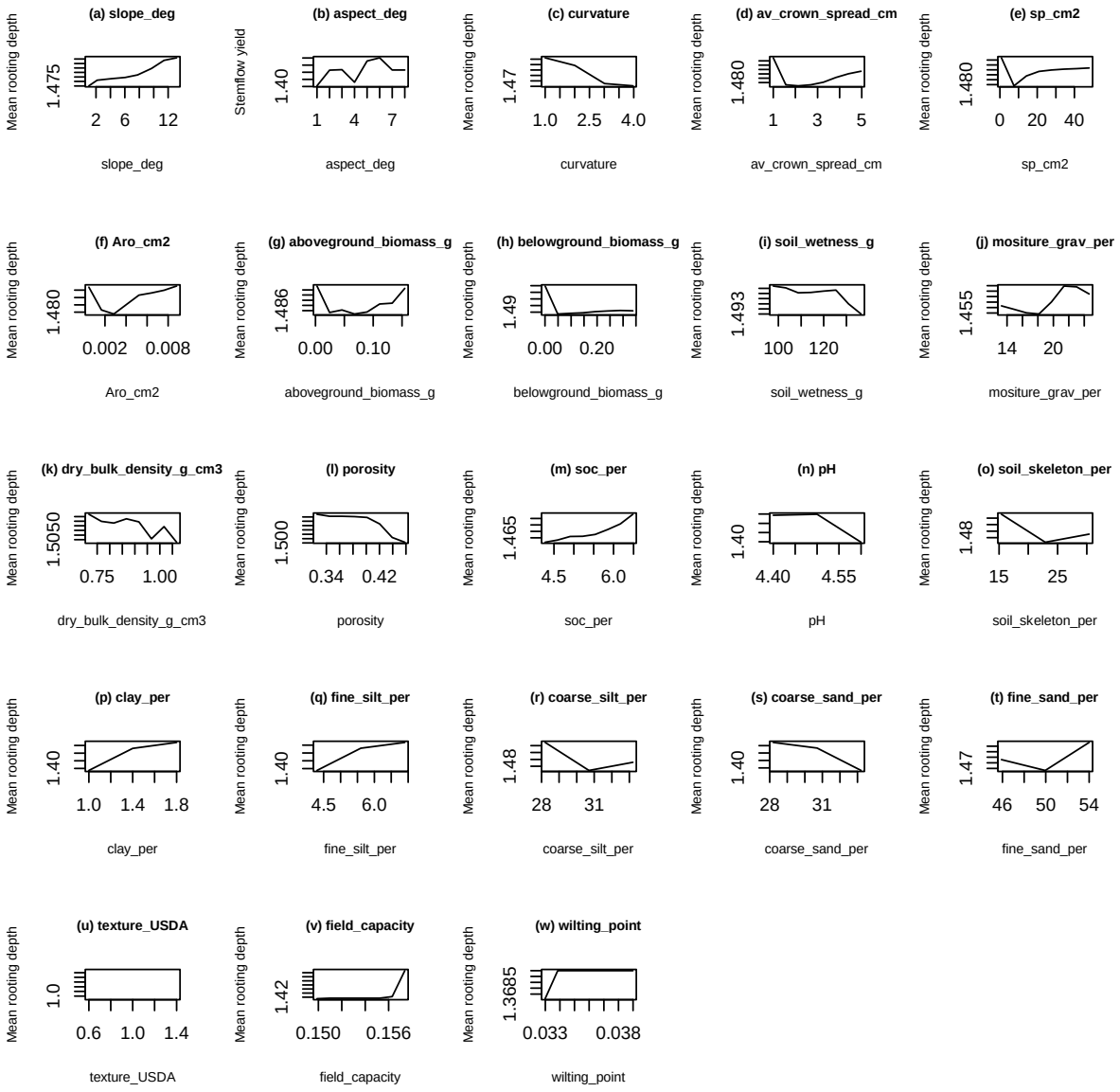

Figure B1. Partial dependence plots (PDPs) showing the relationship between the mean rooting depth (b) and the investigated plant and soil attributes in this study retrieved from fitting random forest models as indicated in the analytical framework shown in Figure 4.

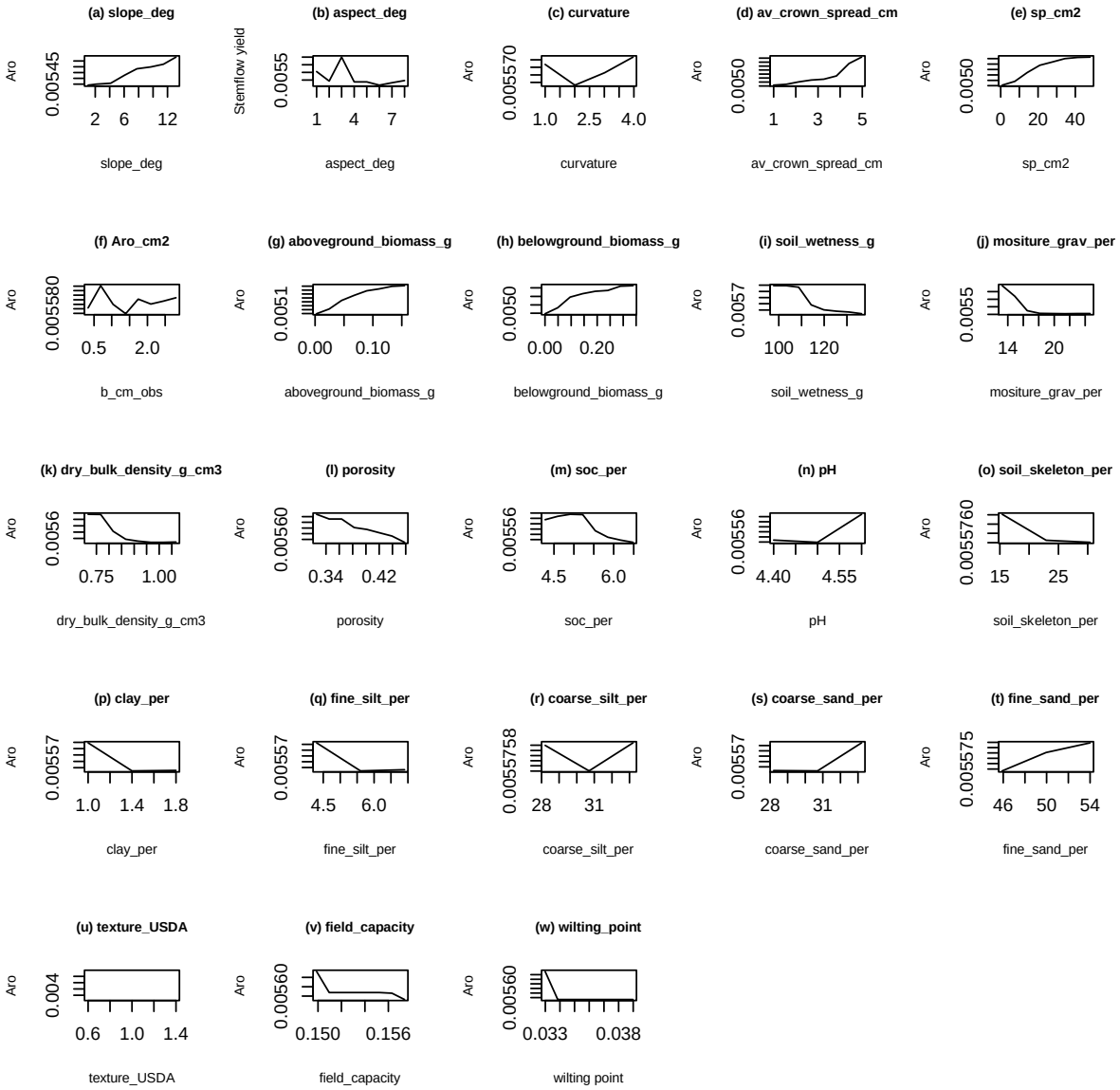

Figure B2. Partial dependence plots (PDPs) showing the relationship between the cross-sectional area at the root collar (Aro) and the investigated plant and soil attributes in this study retrieved from fitting random forest models as indicated in the analytical framework shown in Figure 4.

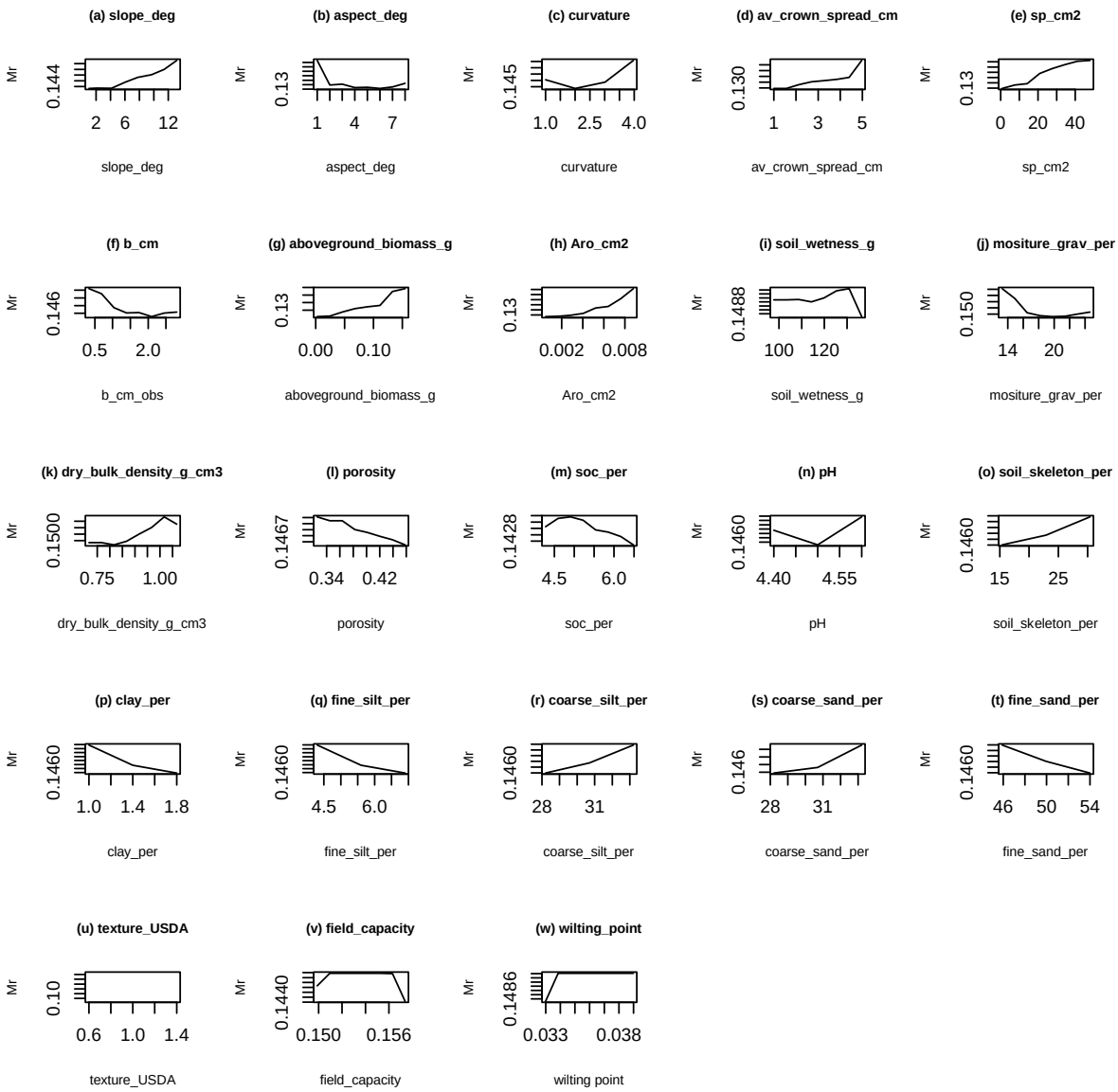

Figure B3. Partial dependence plots (PDPs) showing the relationship between the root biomass (Mr) and the investigated plant and soil attributes in this study retrieved from fitting random forest models as indicated in the analytical framework shown Figure 4.

Appendix C. R script – VRD data mining

```
#Description:
#this script provides a series of functions to evaluate the relationship between the 'rooting
 depth' variable and selected soil and plant attributes. Please, note that this is just a
 sample script for the 'rooting depth' only.
#Instructions:
#copy-paste the following script in your R console https://cran.r-project.org/ and change the
 working directory as appropriate
#########################################################
#Outline
#########
#i-RANDOM FOREST IMPLEMENTATION: it fits random forest models (RF) between the target
 variable and selected plant and soil attributes and generates data frames storing relevant
 outputs related to goodness of fit and relative importance of covariates
#ii-OUTPUTS COLLECTION AND RELATIVE IMPORTANCE EVALUATION: outputs collection, generation of
 output datasets and creation of relevant plots evaluating model quality
#iii-PARTIAL DEPENDENCE PLOTS: creates practical dependence plots for the target variable
#############################################################################################
#Abbreviations:

#b_cm_obs: measured mean rooting depth in cm
#############################################


#load data set and required R packages

setwd("/Users/ollauri/Desktop/work/catena_roots/in") #write the path to your folder here
dts<-read.csv("DATASET.csv")
library(caret)
library(rattle)
library(pdp)
library(randomForest)

#~~~~~~~~~~~~~~~~~~~~~~~~~~~~~~~~~
#i: RANDOM FOREST IMPLEMENTATION
#~~~~~~~~~~~~~~~~~~~~~~~~~~~~~~~~~


n<-100 #number of models to fit
RFs.b<-vector("list",n) #empty list object to store RF models
predictions.b<-vector("list",n) #empty list object to store predictions from RF models
train.A<-vector("list",n) #empty list object to store train data sets to fit RFs
LMs.b<-vector("list",n) #empty list object to store objective function -i.e. linear
 regression models between observed and predicted
RMSEs.b<-vector("list",n) #empty list to store RMSE (root mean square error)
Rsq.b<-vector("list",n) #empty list to store coefficient of determination (r-sq)
out.b<-list() #empty list to store outputs
ct<-seq(1,100) #vector to assign numbers to outputs
output.b<-matrix(,nrow=n,ncol=3) #empty matrix to store outputs
varImp.b<-vector("list",n) #empty list to store variables importance
varImp.vals.b<-list() #empty list to store values of relative importance
varImp.names.b<-list() #empty list to sotore variables names related to relative importance
for(i in 1:n){
 set.seed(i) #random number changes in each model run
 train.A[[i]]<-sample(nrow(dts),0.7*nrow(dts)) #sets training data set - i.e. bootstrapping
 RFs.b[[i]]<-randomForest(b_cm_obs~species+site+slope_deg+aspect_deg+curvature+
 av_crown_spread_cm+ sp_cm2+ Aro_cm2+aboveground_biomass_g+belowground_biomass_g+
 soil_wetness_g+ mositure_grav_per+ dry_bulk_density_g_cm3+ porosity+ soc_per+ pH+
 soil_skeleton_per+ clay_per+ fine_silt_per+ coarse_silt_per+ coarse_sand_per+ fine_sand_per+
 texture_USDA+ field_capacity+
 wilting_point,data=dts[train.A[[i]],],mtry=5,importance=TRUE,ntree=1000) #fits random forest
 models between target variable and soil & plant attributes
 predictions.b[[i]]<-predict(RFs.b[[i]],dts[-train.A[[i]],]) #predictions using the RF models
 and remaining data set
 LMs.b[[i]]<-lm(predictions.b[[i]]~dts$b_cm_obs[-train.A[[i]]]) #fits regression models
 RMSEs.b[[i]]<-sqrt(mean((dts$b_cm_obs[-train.A[[i]]]-predictions.b[[i]])^2)) #calculates RMSE
 Rsq.b[[i]]<-as.matrix(summary(LMs.b[[i]])$adj.r.squared) #calculates r-sq
 out.b[[i]]<-list(ct[i],Rsq.b[[i]],RMSEs.b[[i]]) #stores outputs
 output.b[i,]<-c(out.b[[i]][[1]],as.numeric(out.b[[i]][[2]]),out.b[[i]][[3]]) #arranges
 outputs
 varImp.b[[i]]<-varImp(RFs.b[[i]]) #calculates RELATIVE IMPORTANCE
```

```
 varImp.vals.b[[i]]<-varImp.b[[i]] #stores relative importance values
 varImp.names.b[[i]]<-rownames(varImp.b[[i]])#stores variables names
}


#~~~~~~~~~~~~~~~~~~~~~~~~~~~~~~~~
#ii: OUTPUTS COLLECTION
#~~~~~~~~~~~~~~~~~~~~~~~~~~~~~~~~
setwd("/Users/ollauri/Desktop/work/catena_roots/out")
pdf("RFs_hist_rooting_depth_global.pdf")
hist(output.b[,2],col="gray",main="b vs plant &
 soil",xlab=expression(paste("R"^"2")),ylim=c(0,40)) #histogram showing density distribution
 function for goodness of fit of RF models
dev.off()
out.df.b<-data.frame(model=output.b[,1],Rsq=output.b[,2],RMSE=output.b[,3])
write.csv(out.df.b,"b_global_RFs.csv") #data frame storing summary for RF models' goodness of
 fit
save(RFs.b,file="RFs_b_global.RData") #data base storing RF models
varImp.df.b<-data.frame(var=unlist(varImp.names.b),imp=unlist(varImp.vals.b))
write.csv(varImp.df.b,"varImp_b.csv") #data frame storing relative influence
pdf("RFs_b_varImp.pdf")
boxplot(imp~reorder(var,imp,FUN=mean),data=varImp.df.b,horizontal=TRUE,las=2,cex.axis=0.7,mai
 n="varImp rooting depth") #boxplot for relative influence
dev.off()




#~~~~~~~~~~~~~~~~~~~~~~~~~~~~~~~~
#iii:PARTIAL DEPENDENCE PLOTS
#~~~~~~~~~~~~~~~~~~~~~~~~~~~~~~~~

#Note: numerical variables, only - factor/character must be coded into numeric variables
 first


#p1.x<-vector("list",n) #empty vectors to store partial dependence
p2.x<-vector("list",n)
p3.x<-vector("list",n)
#p4.x<-vector("list",n)
#p5.x<-vector("list",n)
p6.x<-vector("list",n)
p7.x<-vector("list",n)
p8.x<-vector("list",n)
p9.x<-vector("list",n)
p10.x<-vector("list",n)
p11.x<-vector("list",n)
p12.x<-vector("list",n)
p13.x<-vector("list",n)
p14.x<-vector("list",n)
p15.x<-vector("list",n)
p16.x<-vector("list",n)
p17.x<-vector("list",n)
p18.x<-vector("list",n)
p19.x<-vector("list",n)
p20.x<-vector("list",n)
p21.x<-vector("list",n)
p22.x<-vector("list",n)
#p23.x<-vector("list",n)
p24.x<-vector("list",n)
p25.x<-vector("list",n)

#store partial dependence for each covariate with the target variable
for(i in 1:n){
#p1.x[[i]]<-partial(RFs.b[[i]],pred.var="species",plot=FALSE,from=0,to=10)
p2.x[[i]]<-partial(RFs.b[[i]],pred.var="site",plot=FALSE)
p3.x[[i]]<-partial(RFs.b[[i]],pred.var="slope_deg",plot=FALSE)
#p4.x[[i]]<-partial(RFs.b[[i]],pred.var="aspect_deg",plot=FALSE)
#p5.x[[i]]<-partial(RFs.b[[i]],pred.var="curvature",plot=FALSE)
p6.x[[i]]<-partial(RFs.b[[i]],pred.var="av_crown_spread_cm",plot=FALSE)
p7.x[[i]]<-partial(RFs.b[[i]],pred.var="sp_cm2",plot=FALSE)
p8.x[[i]]<-partial(RFs.b[[i]],pred.var="Aro_cm2",plot=FALSE)
p9.x[[i]]<-partial(RFs.b[[i]],pred.var="aboveground_biomass_g",plot=FALSE)
p10.x[[i]]<-partial(RFs.b[[i]],pred.var="belowground_biomass_g",plot=FALSE)
p11.x[[i]]<-partial(RFs.b[[i]],pred.var="soil_wetness_g",plot=FALSE)
```

```
p12.x[[i]]<-partial(RFs.b[[i]],pred.var="mositure_grav_per",plot=FALSE)
p13.x[[i]]<-partial(RFs.b[[i]],pred.var="dry_bulk_density_g_cm3",plot=FALSE)
p14.x[[i]]<-partial(RFs.b[[i]],pred.var="porosity",plot=FALSE)
p15.x[[i]]<-partial(RFs.b[[i]],pred.var="soc_per",plot=FALSE)
p16.x[[i]]<-partial(RFs.b[[i]],pred.var="pH",plot=FALSE)
p17.x[[i]]<-partial(RFs.b[[i]],pred.var="soil_skeleton_per",plot=FALSE)
p18.x[[i]]<-partial(RFs.b[[i]],pred.var="clay_per",plot=FALSE)
p19.x[[i]]<-partial(RFs.b[[i]],pred.var="fine_silt_per",plot=FALSE)
p20.x[[i]]<-partial(RFs.b[[i]],pred.var="coarse_silt_per",plot=FALSE)
p21.x[[i]]<-partial(RFs.b[[i]],pred.var="coarse_sand_per",plot=FALSE)
p22.x[[i]]<-partial(RFs.b[[i]],pred.var="fine_sand_per",plot=FALSE)
#p23.x[[i]]<-partial(RFs.b[[i]],pred.var="texture_USDA",plot=FALSE)
p24.x[[i]]<-partial(RFs.b[[i]],pred.var="field_capacity",plot=FALSE)
p25.x[[i]]<-partial(RFs.b[[i]],pred.var="wilting_point",plot=FALSE)
}

#retrieve outputs and arrange them for graphic display

#p1.a<-list()
#for(i in 1:n){
#      p1.a[[i]]<-p1.x[[i]][[1]]
#}
#p1.mtx.a<-do.call(rbind,p1.a)
#p1.mtx.a.t<-t(p1.mtx.a)
#p1.xs<-rowMeans(p1.mtx.a.t)
#p1.b<-list()
#for(i in 1:n){
 #p1.b[[i]]<-p1.x[[i]][[2]]
#}

#p1.mtx<-do.call(rbind,p1.b) #i kind of have now the list elements in a matrix
#p1.mtx.t<-t(p1.mtx)
#p1.yhat<-rowMeans(p1.mtx.t)

p2.a<-list()
for(i in 1:n){
 p2.a[[i]]<-p2.x[[i]][[1]]
}
p2.mtx.a<-do.call(rbind,p2.a)
p2.mtx.a.t<-t(p2.mtx.a)
p2.xs<-rowMeans(p2.mtx.a.t)
p2.b<-list()
for(i in 1:n){
 p2.b[[i]]<-p2.x[[i]][[2]]
}
p2.mtx<-do.call(rbind,p2.b)
p2.mtx.t<-t(p2.mtx)
p2.yhat<-rowMeans(p2.mtx.t)

p3.a<-list()
for(i in 1:n){
 p3.a[[i]]<-p3.x[[i]][[1]]
}
p3.mtx.a<-do.call(rbind,p3.a)
p3.mtx.a.t<-t(p3.mtx.a)
p3.xs<-rowMeans(p3.mtx.a.t)
p3.b<-list()
for(i in 1:n){
 p3.b[[i]]<-p3.x[[i]][[2]]
}
p3.mtx<-do.call(rbind,p3.b)
p3.mtx.t<-t(p3.mtx)
p3.yhat<-rowMeans(p3.mtx.t)

#p4.a<-list()
#for(i in 1:n){
#      p4.a[[i]]<-p4.x[[i]][[1]]
#}
#p4.mtx.a<-do.call(rbind,p4.a)
#p4.mtx.a.t<-t(p4.mtx.a)
#p4.xs<-rowMeans(p4.mtx.a.t)
#p4.b<-list()
#for(i in 1:n){
#      p4.b[[i]]<-p4.x[[i]][[2]]
#}
#p4.mtx<-do.call(rbind,p4.b)
#p4.mtx.t<-t(p4.mtx)
```

```
#p4.yhat<-rowMeans(p4.mtx.t)

#p5.a<-list()
#for(i in 1:n){
#      p5.a[[i]]<-p5.x[[i]][[1]]
#}
#p5.mtx.a<-do.call(rbind,p5.a)
#p5.mtx.a.t<-t(p5.mtx.a)
#p5.xs<-rowMeans(p5.mtx.a.t)
#p5.b<-list()
#for(i in 1:n){
#      p5.b[[i]]<-p5.x[[i]][[2]]
#}
#p5.mtx<-do.call(rbind,p5.b)
#p5.mtx.t<-t(p5.mtx)
#p5.yhat<-rowMeans(p5.mtx.t)

p6.a<-list()
for(i in 1:n){
 p6.a[[i]]<-p6.x[[i]][[1]]
}
p6.mtx.a<-do.call(rbind,p6.a)
p6.mtx.a.t<-t(p6.mtx.a)
p6.xs<-rowMeans(p6.mtx.a.t)
p6.b<-list()
for(i in 1:n){
 p6.b[[i]]<-p6.x[[i]][[2]]
}
p6.mtx<-do.call(rbind,p6.b)
p6.mtx.t<-t(p6.mtx)
p6.yhat<-rowMeans(p6.mtx.t)

p7.a<-list()
for(i in 1:n){
 p7.a[[i]]<-p7.x[[i]][[1]]
}
p7.mtx.a<-do.call(rbind,p7.a)
p7.mtx.a.t<-t(p7.mtx.a)
p7.xs<-rowMeans(p7.mtx.a.t)
p7.b<-list()
for(i in 1:n){
 p7.b[[i]]<-p7.x[[i]][[2]]
}
p7.mtx<-do.call(rbind,p7.b)
p7.mtx.t<-t(p7.mtx)
p7.yhat<-rowMeans(p7.mtx.t)

p8.a<-list()
for(i in 1:n){
 p8.a[[i]]<-p8.x[[i]][[1]]
}
p8.mtx.a<-do.call(rbind,p8.a)
p8.mtx.a.t<-t(p8.mtx.a)
p8.xs<-rowMeans(p8.mtx.a.t)
p8.b<-list()
for(i in 1:n){
 p8.b[[i]]<-p8.x[[i]][[2]]
}
p8.mtx<-do.call(rbind,p8.b)
p8.mtx.t<-t(p8.mtx)
p8.yhat<-rowMeans(p8.mtx.t)

p9.a<-list()
for(i in 1:n){
 p9.a[[i]]<-p9.x[[i]][[1]]
}
p9.mtx.a<-do.call(rbind,p9.a)
p9.mtx.a.t<-t(p9.mtx.a)
p9.xs<-rowMeans(p9.mtx.a.t)
p9.b<-list()
for(i in 1:n){
 p9.b[[i]]<-p9.x[[i]][[2]]
}
p9.mtx<-do.call(rbind,p9.b)
p9.mtx.t<-t(p9.mtx)
p9.yhat<-rowMeans(p9.mtx.t)
```

```
p10.a<-list()
for(i in 1:n){
 p10.a[[i]]<-p10.x[[i]][[1]]
}
p10.mtx.a<-do.call(rbind,p10.a)
p10.mtx.a.t<-t(p10.mtx.a)
p10.xs<-rowMeans(p10.mtx.a.t)
p10.b<-list()
for(i in 1:n){
 p10.b[[i]]<-p10.x[[i]][[2]]
}
p10.mtx<-do.call(rbind,p10.b)
p10.mtx.t<-t(p10.mtx)
p10.yhat<-rowMeans(p10.mtx.t)

p11.a<-list()
for(i in 1:n){
 p11.a[[i]]<-p11.x[[i]][[1]]
}
p11.mtx.a<-do.call(rbind,p11.a)
p11.mtx.a.t<-t(p11.mtx.a)
p11.xs<-rowMeans(p11.mtx.a.t)
p11.b<-list()
for(i in 1:n){
 p11.b[[i]]<-p11.x[[i]][[2]]
}
p11.mtx<-do.call(rbind,p11.b)
p11.mtx.t<-t(p11.mtx)
p11.yhat<-rowMeans(p11.mtx.t)

p12.a<-list()
for(i in 1:n){
 p12.a[[i]]<-p12.x[[i]][[1]]
}
p12.mtx.a<-do.call(rbind,p12.a)
p12.mtx.a.t<-t(p12.mtx.a)
p12.xs<-rowMeans(p12.mtx.a.t)
p12.b<-list()
for(i in 1:n){
 p12.b[[i]]<-p12.x[[i]][[2]]
}
p12.mtx<-do.call(rbind,p12.b)
p12.mtx.t<-t(p12.mtx)
p12.yhat<-rowMeans(p12.mtx.t)

p13.a<-list()
for(i in 1:n){
 p13.a[[i]]<-p13.x[[i]][[1]]
}
p13.mtx.a<-do.call(rbind,p13.a)
p13.mtx.a.t<-t(p13.mtx.a)
p13.xs<-rowMeans(p13.mtx.a.t)
p13.b<-list()
for(i in 1:n){
 p13.b[[i]]<-p13.x[[i]][[2]]
}
p13.mtx<-do.call(rbind,p13.b)
p13.mtx.t<-t(p13.mtx)
p13.yhat<-rowMeans(p13.mtx.t)

p14.a<-list()
for(i in 1:n){
 p14.a[[i]]<-p14.x[[i]][[1]]
}
p14.mtx.a<-do.call(rbind,p14.a)
p14.mtx.a.t<-t(p14.mtx.a)
p14.xs<-rowMeans(p14.mtx.a.t)
p14.b<-list()
for(i in 1:n){
 p14.b[[i]]<-p14.x[[i]][[2]]
}
p14.mtx<-do.call(rbind,p14.b)
p14.mtx.t<-t(p14.mtx)
p14.yhat<-rowMeans(p14.mtx.t)

p15.a<-list()
for(i in 1:n){
```

```
 p15.a[[i]]<-p15.x[[i]][[1]]
}
p15.mtx.a<-do.call(rbind,p15.a)
p15.mtx.a.t<-t(p15.mtx.a)
p15.xs<-rowMeans(p15.mtx.a.t)
p15.b<-list()
for(i in 1:n){
 p15.b[[i]]<-p15.x[[i]][[2]]
}
p15.mtx<-do.call(rbind,p15.b)
p15.mtx.t<-t(p15.mtx)
p15.yhat<-rowMeans(p15.mtx.t)


p16.a<-list()
for(i in 1:n){
 p16.a[[i]]<-p16.x[[i]][[1]]
}
p16.mtx.a<-do.call(rbind,p16.a)
p16.mtx.a.t<-t(p16.mtx.a)
p16.xs<-rowMeans(p16.mtx.a.t)
p16.b<-list()
for(i in 1:n){
 p16.b[[i]]<-p16.x[[i]][[2]]
}
p16.mtx<-do.call(rbind,p16.b)
p16.mtx.t<-t(p16.mtx)
p16.yhat<-rowMeans(p16.mtx.t)

p17.a<-list()
for(i in 1:n){
 p17.a[[i]]<-p17.x[[i]][[1]]
}
p17.mtx.a<-do.call(rbind,p17.a)
p17.mtx.a.t<-t(p17.mtx.a)
p17.xs<-rowMeans(p17.mtx.a.t)
p17.b<-list()
for(i in 1:n){
 p17.b[[i]]<-p17.x[[i]][[2]]
}
p17.mtx<-do.call(rbind,p17.b)
p17.mtx.t<-t(p17.mtx)
p17.yhat<-rowMeans(p17.mtx.t)

p18.a<-list()
for(i in 1:n){
 p18.a[[i]]<-p18.x[[i]][[1]]
}
p18.mtx.a<-do.call(rbind,p18.a)
p18.mtx.a.t<-t(p18.mtx.a)
p18.xs<-rowMeans(p18.mtx.a.t)
p18.b<-list()
for(i in 1:n){
 p18.b[[i]]<-p18.x[[i]][[2]]
}
p18.mtx<-do.call(rbind,p18.b)
p18.mtx.t<-t(p18.mtx)
p18.yhat<-rowMeans(p18.mtx.t)

p19.a<-list()
for(i in 1:n){
 p19.a[[i]]<-p19.x[[i]][[1]]
}
p19.mtx.a<-do.call(rbind,p19.a)
p19.mtx.a.t<-t(p19.mtx.a)
p19.xs<-rowMeans(p19.mtx.a.t)
p19.b<-list()
for(i in 1:n){
 p19.b[[i]]<-p19.x[[i]][[2]]
}
p19.mtx<-do.call(rbind,p19.b)
p19.mtx.t<-t(p19.mtx)
p19.yhat<-rowMeans(p19.mtx.t)

p20.a<-list()
for(i in 1:n){
 p20.a[[i]]<-p20.x[[i]][[1]]
```

```
}
p20.mtx.a<-do.call(rbind,p20.a)
p20.mtx.a.t<-t(p20.mtx.a)
p20.xs<-rowMeans(p20.mtx.a.t)
p20.b<-list()
for(i in 1:n){
 p20.b[[i]]<-p20.x[[i]][[2]]
}
p20.mtx<-do.call(rbind,p20.b)
p20.mtx.t<-t(p20.mtx)
p20.yhat<-rowMeans(p20.mtx.t)

p21.a<-list()
for(i in 1:n){
 p21.a[[i]]<-p21.x[[i]][[1]]
}
p21.mtx.a<-do.call(rbind,p21.a)
p21.mtx.a.t<-t(p21.mtx.a)
p21.xs<-rowMeans(p21.mtx.a.t)
p21.b<-list()
for(i in 1:n){
 p21.b[[i]]<-p21.x[[i]][[2]]
}
p21.mtx<-do.call(rbind,p21.b)
p21.mtx.t<-t(p21.mtx)
p21.yhat<-rowMeans(p21.mtx.t)

p22.a<-list()
for(i in 1:n){
 p22.a[[i]]<-p22.x[[i]][[1]]
}
p22.mtx.a<-do.call(rbind,p22.a)
p22.mtx.a.t<-t(p22.mtx.a)
p22.xs<-rowMeans(p22.mtx.a.t)
p22.b<-list()
for(i in 1:n){
 p22.b[[i]]<-p22.x[[i]][[2]]
}
p22.mtx<-do.call(rbind,p22.b)
p22.mtx.t<-t(p22.mtx)
p22.yhat<-rowMeans(p22.mtx.t)

#p23.a<-list()
#for(i in 1:n){
#      p23.a[[i]]<-p23.x[[i]][[1]]
#}
#p23.mtx.a<-do.call(rbind,p23.a)
#p23.mtx.a.t<-t(p23.mtx.a)
#p23.xs<-rowMeans(p23.mtx.a.t)
#p23.b<-list()
#for(i in 1:n){
#      p23.b[[i]]<-p23.x[[i]][[2]]
#}
#p23.mtx<-do.call(rbind,p23.b)
#p23.mtx.t<-t(p23.mtx)
#p23.yhat<-rowMeans(p23.mtx.t)

p24.a<-list()
for(i in 1:n){
 p24.a[[i]]<-p24.x[[i]][[1]]
}
p24.mtx.a<-do.call(rbind,p24.a)
p24.mtx.a.t<-t(p24.mtx.a)
p24.xs<-rowMeans(p24.mtx.a.t)
p24.b<-list()
for(i in 1:n){
 p24.b[[i]]<-p24.x[[i]][[2]]
}
p24.mtx<-do.call(rbind,p24.b)
p24.mtx.t<-t(p24.mtx)
p24.yhat<-rowMeans(p24.mtx.t)

p25.a<-list()
for(i in 1:n){
 p25.a[[i]]<-p25.x[[i]][[1]]
}
p25.mtx.a<-do.call(rbind,p25.a)
```

```
p25.mtx.a.t<-t(p25.mtx.a)
p25.xs<-rowMeans(p25.mtx.a.t)
p25.b<-list()
for(i in 1:n){
 p25.b[[i]]<-p25.x[[i]][[2]]
}
p25.mtx<-do.call(rbind,p25.b)
p25.mtx.t<-t(p25.mtx)
p25.yhat<-rowMeans(p25.mtx.t)

#plot PDPs


pdf("RFs_rooting_depth_PDPs.pdf")
par(mfrow=c(5,5))
#plot(p1.yhat[1:8]~p1.xs[1:8],type="l",xlab="species",ylab="Mean rooting depth",main="(a)
 species",cex.main=0.8,cex.lab=0.8)
plot(p2.yhat[1:8]~p2.xs[1:8],type="l",xlab="site",ylab="Mean rooting depth",main="(b)
 site",cex.main=0.8,cex.lab=0.8)
plot(p3.yhat[1:8]~p3.xs[1:8],type="l",xlab="slope_deg",ylab="Mean rooting depth",main="(c)
 slope_deg",cex.main=0.8,cex.lab=0.8)
#plot(p4.yhat[1:8]~p4.xs[1:8],type="l",xlab="aspect_deg",ylab="Mean rooting depth",main="(d)
 aspect_deg",cex.main=0.8,cex.lab=0.8)
#plot(p5.yhat[1:8]~p5.xs[1:8],type="l",xlab="curvature",ylab="Mean rooting depth",main="(e)
 curvature",cex.main=0.8,cex.lab=0.8)
plot(p6.yhat[1:8]~p6.xs[1:8],type="l",xlab="av_crown_spread_cm",ylab="Mean rooting
 depth",main="(f) av_crown_spread_cm",cex.main=0.8,cex.lab=0.8)
plot(p7.yhat[1:8]~p7.xs[1:8],type="l",xlab="sp_cm2",ylab="Mean rooting depth",main="(g)
 sp_cm2",cex.main=0.8,cex.lab=0.8)
plot(p8.yhat[1:8]~p8.xs[1:8],type="l",xlab="Aro_cm2",ylab="Mean rooting depth",main="(h)
 Aro_cm2",cex.main=0.8,cex.lab=0.8)
plot(p9.yhat[1:8]~p9.xs[1:8],type="l",xlab="aboveground_biomass_g",ylab="Mean rooting
 depth",main="(i) aboveground_biomass_g",cex.main=0.8,cex.lab=0.8)
plot(p10.yhat[1:8]~p10.xs[1:8],type="l",xlab="belowground_biomass_g",ylab="Mean rooting
 depth",main="(j) belowground_biomass_g",cex.main=0.8,cex.lab=0.8)
plot(p11.yhat[1:8]~p11.xs[1:8],type="l",xlab="soil_wetness_g",ylab="Mean rooting
 depth",main="(k) soil_wetness_g",cex.main=0.8,cex.lab=0.8)
plot(p12.yhat[1:8]~p12.xs[1:8],type="l",xlab="mositure_grav_per",ylab="Mean rooting
 depth",main="(l) mositure_grav_per",cex.main=0.8,cex.lab=0.8)
plot(p13.yhat[1:8]~p13.xs[1:8],type="l",xlab="dry_bulk_density_g_cm3",ylab="Mean rooting
 depth",main="(m) dry_bulk_density_g_cm3",cex.main=0.8,cex.lab=0.8)
plot(p14.yhat[1:8]~p14.xs[1:8],type="l",xlab="porosity",ylab="Mean rooting depth",main="(n)
 porosity",cex.main=0.8,cex.lab=0.8)
plot(p15.yhat[1:8]~p15.xs[1:8],type="l",xlab="soc_per",ylab="Mean rooting depth",main="(o)
 soc_per",cex.main=0.8,cex.lab=0.8)
plot(p16.yhat[1:8]~p16.xs[1:8],type="l",xlab="pH",ylab="Mean rooting depth",main="(p)
 pH",cex.main=0.8,cex.lab=0.8)
plot(p17.yhat[1:8]~p17.xs[1:8],type="l",xlab="soil_skeleton_per",ylab="Mean rooting
 depth",main="(p) soil_skeleton_per",cex.main=0.8,cex.lab=0.8)
plot(p18.yhat[1:8]~p18.xs[1:8],type="l",xlab="clay_per",ylab="Mean rooting depth",main="(p)
 clay_per",cex.main=0.8,cex.lab=0.8)
plot(p19.yhat[1:8]~p19.xs[1:8],type="l",xlab="fine_silt_per",ylab="Mean rooting
 depth",main="(p) fine_silt_per",cex.main=0.8,cex.lab=0.8)
plot(p20.yhat[1:8]~p21.xs[1:8],type="l",xlab="coarse_silt_per",ylab="Mean rooting
 depth",main="(p) coarse_silt_per",cex.main=0.8,cex.lab=0.8)
plot(p21.yhat[1:8]~p21.xs[1:8],type="l",xlab="coarse_sand_per",ylab="Mean rooting
 depth",main="(p) coarse_sand_per",cex.main=0.8,cex.lab=0.8)
plot(p22.yhat[1:8]~p22.xs[1:8],type="l",xlab="fine_sand_per",ylab="Mean rooting
 depth",main="(p) fine_sand_per",cex.main=0.8,cex.lab=0.8)
#plot(p23.yhat[1:8]~p23.xs[1:8],type="l",xlab="texture_USDA",ylab="Mean rooting
 depth",main="(p) texture_USDA",cex.main=0.8,cex.lab=0.8)
plot(p24.yhat[1:8]~p24.xs[1:8],type="l",xlab="field_capacity",ylab="Mean rooting
 depth",main="(p) field_capacity",cex.main=0.8,cex.lab=0.8)
plot(p25.yhat[1:8]~p25.xs[1:8],type="l",xlab="wilting_point",ylab="Mean rooting
 depth",main="(p) wilting_point",cex.main=0.8,cex.lab=0.8)
dev.off()
```